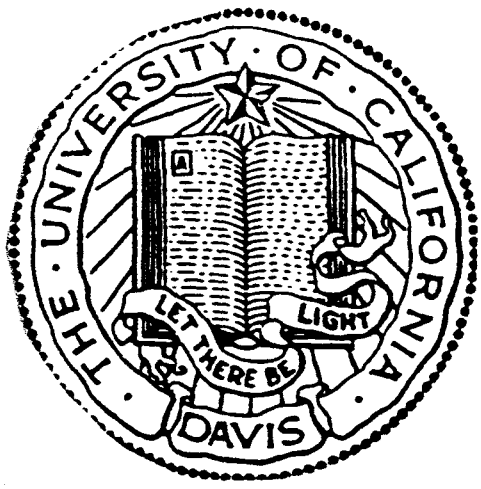

MODELING AND DESIGN ANALYSIS METHODOLOGY FOR TAILORING OF AIRCRAFT STRUCTURES WITH COMPOSITES

By

Lawrence W. Rehfield, Professor
Mechanical and Aeronautical Engineering
One Shields Avenue
University of California, Davis
Davis, California 95616-5294
(530)752-8100
email:lwrehfield@ucdavis.edu

Grant NAG-1-01116
Final Report
NASA Langley Research Center
Mechanics and Durability Branch
MS 188E, Building 1205, Room 103
Hampton, VA 23681-0001

Introduction

Composite materials provide design flexibility in that fiber placement and orientation can be specified and a variety of material forms and manufacturing processes are available. It is possible, therefore, to "tailor" the structure to a high degree in order to meet specific design requirements in an optimum manner. Common industrial practices, however, have limited the choices designers make. One of the reasons for this is that there is a dearth of conceptual/preliminary design analysis tools specifically devoted to identifying structural concepts for composite airframe structures. Large scale finite element simulations are not suitable for such purposes.

The present project has been devoted to creating modeling and design analysis methodology for use in the tailoring process of aircraft structures. Emphasis has been given to creating bend-twist elastic coupling in high aspect ratio wings or other lifting surfaces. The direction of our work was in concert with the overall NASA effort Twenty-First Century Aircraft Technology (TCAT). A multi-disciplinary team was assembled by Dr. Damodar Ambur to work on wing technology, which included our project.

Summary of Accomplishments

Our current work has included the following items:

(1) Analysis to design elastically tailored wings with bend-twist coupling one cross section at a time. This work appears in Appendix I.

Tapered wings may be analyzed with the use of item (1) to discrete spanwise wing stations and with the loads known. Our grant monitor, Dr. Damodar Ambur, redirected us in 2003 to put a special emphasis on making the analysis of highly

tapered wings a significant priority and to make it efficient. The result is in items (2) and (3).

(2) Analysis of 3D wings with geometric taper, which includes variation of chord, airfoil thickness and cover wall thickness has been created and applied without bend twist coupling in the wing.

(3) Use of simplified design criteria which include the following steps:

  (a) The wing cover thicknesses are defined by spanwise bending strain level. This is followed by a check for torsional divergence.

  (b) "Rigid" wing loads are used to predict first order elastic deformations.

  (c) Loading redistributions due to first order elastic deformations are evaluated. Effect on bending strain is assessed.

Use the results of (b) and (c) to set composite ply layups in the wing covers for "best" results. This will necessitate subdividing the wing planform into zones of constant ply layups. The zones influence the manufacturing process, and, therefore, require practical judgment.

Iteration may be required to define the cover preliminary thickness estimate. Items (1) and (2) are complete. Item (3) has been conceived and applied to a fictitious Reno Air Racer with no elastic coupling in the wings, but not compared with other methodology such as indicated in item (1).

The differences among (1),(2), and (3) is that (1) requires only structures and materials technology. Item (2) and (3) require aerodynamic and mass information. Also,We have employed aerodynamic strip theory, which lacks 3D resolution, but which

should provide reliable preliminary design definition for the structural configuration. This work appears in Appendix II.

All of our work has been devoted to preliminary design analysis. The objective is to give the designer guidance in establishing the structural configuration. Once a viable configuration is identified, "fine tuning" to save weight and cost can proceed with the aid of large scale numerical simulation and perhaps, in addition, optimization. The key element is the definition of the ply layups.

Concluding Remarks

The effort that we directed to highly tapered wings at Dr. Ambur's suggestion did not permit an evaluation of both taper and bend-twist elastic coupling. A request for additional supplemental funding and additional time was submitted to NASA Langley in order to reach all objectives. Unfortunately, the TCAT program was cancelled and no supplementary funds were provided.

Two Journal of Aircraft papers were written and presented at AIAA conferences. Both papers have been accepted for publication and are under revision. A complete record of the project accomplishments appears in Appendices I and II.

Appendix I

Rosita Cheung's
MS Thesis

2002

SOME STRATEGIES FOR CREATING BEND-TWIST COUPLING IN BOX BEAMS

By

ROSITA HIU-YEE CHEUNG

B.S. (University of California, Davis) 2001

THESIS

Submitted in partial satisfaction of the requirements for the degree of

MASTER OF SCIENCE

in

Engineering

in the

OFFICE OF GRADUATE STUDIES

of the

UNIVERSITY OF CALIFORNIA

DAVIS

Approved:

_____

_____

_____

Committee in Charge

2002

NOMENCLATURE

A	Torsional stiffness matrix
a_{12}	Defined in eq. (14)
a_{26}	Defined in eq. (15)
A_{ij}	Laminate membrane stiffnesses for wing box covers, or elements of matrix A
$\bar{C}_{12}$	Effective Poisson's ratio, eq. (22)
$\bar{C}_{26}$	Twist-camber coupling parameter, eq. (23)
C_{ij}	Beam stiffness matrix
C_{44}	Torsional Stiffness, eq. (6)
C_{45}	Coupling Stiffness, eq. (7)
C_{55}	Bending Stiffness, eq. (8)
c_A	Aerodynamic chord
c_S	Chord of wing section structural box
E_{11}	Young's modulus of composite material in fiber diretion
E_{12}	Young's modulus of composite material in transverse direction
G_{12}	In-plane shear modulus
H	Height of wing section structural box
h	Skin thickness of load bearing covers of the wing structural box
h_k	Thickness of k-th ply of a laminate
K_{ij}	Structural box cover stiffnesses
K_{11}	Extensional stiffness, eq. (2)
K_{12}	Shear stiffness, eq. (3)

K_{22}	Extension-shear coupling stiffness, eq. (4)
k_{ij}	Structural box cover stiffnesses per unit skin thickness
k_c	Camber curvature kinematic matrix defined in eq. (21)
M_x	Chordwise bending moment, eq. (17)
M_y	Spanwise bending moment, eq. (18)
N_{xx}	Axial running load due to bending in the wing box covers
N_{xs}	Membrane shear flow or stress resultant
N_{ss}	Circumferential (hoop) membrane stress resultant
$\overline{Q}_{ij}$	Plane stress stiffnesses for each ply of a laminate
$W_{,xx}$	Bending curvature of wing box structural box, eq. (20)
x,y,z	Cartesian coordinates
1,2	Transformed coordinates
β^2	Bend-twist coupling parameter, eq. (10)
β_1^2	Bend-twist coupling parameter for covers only, eq. (11)
ε	Strain in fiber direction
ε_{xx}, ε_{ss}	Components of extensional membrane strain in cell wall
$\varepsilon_{x\psi}$, $\varepsilon_{y\psi}$	Strains in the x_ψ-y_ψ coordinate system
γ_{xs}	Membrane shear strain in cell wall of wing section structural box
$\mu\varepsilon$	microstrain, strain$\times 10^6$
$\phi_{,x}$	Rate of twist of wing box structural box, eq. (19)
ψ	Laminate rotation angle with respect to the axis of the structure

θ	Dominant skin fiber orientation angle

Superscripts

i,j,k	Refers to indices assuming the values 1, 2, 6

Superscripts

fw	Refers to front spar web
k	Refers to identifying index
l	Refers to lower wing box cover
rw	Refers to rear spar web
u	Refers to upper wing box cover

LIST OF FIGURES

INTRODUCTION

Even many years after the invention of fiber-reinforced composite materials, many new uses are being found for them. They are used in many different applications because of their high strength-to-weight ratio, stiffness-to-weight ratio and increased design flexibility. The goal for designing is usually to reduce weight or cost while achieving high performance products. Although composite materials cost more than metal materials, they can produce cost competitive structures.

Elastic tailoring of composite materials utilizes their design flexibility. From Rehfield's definition[1], an appropriate selection of structural concept, fiber orientation, ply stacking sequences and blending of materials can achieve a specific design goal. In past research, elastic tailoring has been used to influence the aerodynamics of the system[2]. This is defined as "aeroelastic tailoring."

From the definition of Shirk, Hertz and Weisshaar[2], "*Aeroelastic tailoring is the embodiment of directional stiffness into an aircraft structural design to control aeroelastic deformation, static or dynamic, in such a fashion as to affect the aerodynamic and structural performance of the aircraft in a beneficial way.*" The example of it is Grumman's X-29 technology demonstrator. The X-29's forward swept wing has high lift-to-drag ratio and increased resistance to torsional divergence.

The focus of the present work is mainly on bend-twist coupling in high aspect ratio wing boxes. This coupling can increase the stability of the aircraft system and resist the tip stall of subsonic wings. Bend-twist coupling is produced by the stiffness of the angle plies, which are the off-axis plies oriented at angles with respect to the bending axis

of the structure. The laminated ply stiffness depends upon the material and fiber orientation. The coupling created by the stiffness can create the desired effect.

Two design strategies are used to understand the bend-twist coupling, which are angle ply rotation and laminate rotation. These two design strategies have been applied to two types of models. One is the ideal tailored box model from Rehfield's work[3], in which only the upper and lower covers are the load-bearing structural elements. The second is similar to the first one but with the additional sides or spar webs being modeled. In the latter model, all elements of the box are load-bearing. After extensive evaluation, the second model is chosen for our study. The first model tends to under estimate torsional stiffness.

An illustration for a large transport wing section is studied to help understand the two design strategies for producing bend-twist coupling.

DESIGN STRATEGIES

Preliminary Remarks

Bend-twist coupling is produced by creating stiffness which is not aligned with the bending axis of the primary structure. In wing covers made of laminated composites, some off-axis plies will serve to produce the desired effect. This is the context which is considered here.

Angle Ply Rotation

In this thesis, two design strategies are considered: Angle Ply Rotation and Laminate Rotation. The angle ply rotation uses axis-oriented plies and an unbalanced set of angle plies. If desired, transverse plies also can be included to increase damage

tolerance. In this method, bend-twist coupling is produced by the unbalanced layup. The angle ply orientation can be varied in order to enhance coupling. As shown in Figure 1, the axial plies stay in the same position but the angle of the unbalanced set of angle plies varies. The angle, θ, rotates with respect to the axial axis of the structure.

Laminate Rotation

The second design strategy is called "Laminate Rotation." This method has been applied to the swept forward wing of the X-29 and the analysis of bend-twist coupling in Ref. 3. This approach chooses an established layup configuration, which includes axial plies and angle plies. Transverse plies also can be included if desired. As shown in Figure 2, the entire laminate is rotated from the x-y coordinate system to the x_ψ-y_ψ coordinate system with respect to the axial axis of the structure. The coordinates natural to the solution of the structure problem are the structure coordinates x, y, whereas the principal material coordinates are x_ψ, y_ψ. The rotation angle, ψ, is the angle measured from the x-axis to the x_ψ-axis. It is recommended to choose a balanced layup configuration in order to avoid or minimize warping due to processing. After the rotation, the plies are no longer aligned with the axis and bend-twist coupling is introduced.

The angle plies in the Angle Ply Rotation method and the laminate in the Laminate Rotation method are rotated until they produce the desired bend-twist coupling. It is efficient to have all angle plies in angle ply rotation to produce bend-twist coupling. However, there is a disadvantage that arises from the common manufacturing-related warping produced by processing thermoset composite materials for unbalanced

configurations. The advantages of angle ply rotation method over the laminate rotation method will inspire innovative utilization. For this method, warping effects due to unbalanced configurations will be neglected.

MODEL AND ANALYSIS

Model

A simple model is employed to analyze the wing box using the two design strategies. This model is based upon a refinement of the one in Ref. 3, which considers load bearing covers and spar webs or sides which are not modeled. The model shown in Fig. 3 is used for this study. It factors in the effects of the webs being modeled. As a result, this model has contributions from every portion of the box. This approach is more realistic. Based upon a consensus of Refs. 4-6, the webs are assumed to be made of balanced angle plies. The preferred choice is [±45] plies[4-6]. In addition, the recommended choice for the web wall thickness is less than half of the covers.

The coordinate system of the box model is shown in Fig. 4, where x and s are indicated. Also, the figure shows the ply orientation for the covers. The upper and lower covers are tailored identically and asymmetrically. They are mirror images of each other, which is the "best" way to create bend-twist coupling. The angle θ is the angle between the dominant off-axis and the ply orientation. The laminates for the upper and lower covers can be made of axial plies, angle plies, and transverse plies. Since the s coordinate surrounds the box model, the signs for the angles are different for the covers. As shown in Fig. 5, the angle for the upper cover is positive, but negative for the lower cover.

Analysis of the Model

The analysis methodology is based upon the Bernoulli-Euler bending assumption applied to Rehfield's theory of thin-walled composite beams[1]. The warping effects and transverse shear deformations are neglected here. The walls of the model carry loads in plane stress, and the stress resultants for the walls are denoted N_{xx}, N_{xs} and N_{ss}. The axial running load due to bending is N_{xx}, and N_{xs} is the running load due to torsion (shear flow). The circumferential stress resultant, N_{ss} is assumed to be negligible. This implies no internal pressure. Consequently,

$$\begin{Bmatrix} N_{xx} \\ N_{xs} \end{Bmatrix} = \begin{bmatrix} K_{11} & K_{12} \\ K_{12} & K_{22} \end{bmatrix} \begin{Bmatrix} \varepsilon_{xx} \\ \gamma_{xs} \end{Bmatrix} \qquad (1)$$

K_{11}, K_{12} and K_{22} corresponds to uniaxial extension, shear, and coupling stiffnesses, respectively. They are defined as

$$K_{11} = A_{11} - \frac{(A_{12})^2}{A_{22}} \qquad (2)$$

$$K_{12} = A_{16} - \frac{A_{16}A_{26}}{A_{22}} \qquad (3)$$

$$K_{22} = A_{66} - \frac{A_{26}^{\ 2}}{A_{22}} \qquad (4)$$

The membrane stiffnesses, A_{ij}, are independent of the stacking sequence, which can be determined by simply adding the plane stress stiffnesses, $\overline{Q}_{ij}$, for each ply. For a laminate of N plies,

$$A_{ij} = \sum_{k=1}^{N} \overline{Q}_{ij}^{(k)} h_k \qquad (i, j = 1, 2, 6) \qquad (5)$$

where h_k is the thickness of k^{th} ply.

Since the webs have contributions of stiffnesses for the present model, the expressions of the global stiffnesses are different from the previous model in Ref. 7. The global stiffnesses are

$$C_{44} = \frac{Cs^2H^2}{(Cs+H)^2}\left[\left(K_{22}{}^{u} + K_{22}{}^{l}\right)Cs + h\left(f_f \bar{Q}_{66}{}^{fw} + f_r \bar{Q}_{66}{}^{rw}\right)H\right] \quad (6)$$

$$C_{45} = \frac{Cs^2H^2}{2(Cs+H)}\left(K_{12}{}^{u} - K_{12}{}^{l}\right) \quad (7)$$

$$C_{55} = \frac{CsH^2}{4}\left(K_{11}{}^{u} + K_{11}{}^{l}\right) \quad (8)$$

where C_{44}, C_{45} and C_{55} are the torsional, coupling, and bending stiffnesses, respectively. In eqs. (6)-(8), the superscripts u and l denote the upper and lower covers, respectively, and fw and rw denote the front and rear spar webs, respectively. The web wall thickness is a fraction of the cover wall thickness, h, which f_f is the fraction for front spar web and f_r is the fraction for the rear spar web.

Since a balanced configuration is chosen for the webs, the coupling stiffness is not affected. Furthermore, the bending effects from the webs are neglected[5]; the only stiffness that is affected is C_{44}, the torsional stiffness, which is increased.

The stiffnesses require the determination of wall thickness by using layup coefficients for a unit thickness in the strain limit equation. It is convenient to define the membrane stiffness in terms of thickness

$$K_{ij} = hk_{ij} \qquad (i, j = 1, 2) \quad (9)$$

and the bend-twist coupling parameters that are convenient to define[3]

$$\beta^2 = (C_{45})^2 \Big/ C_{44}C_{55} \quad (10)$$

$$\beta_1^2 = (K_{12})^2 / K_{11}K_{22} \tag{11}$$

Design Analysis Methodology for Angle Ply Rotation

The design criterion used is to limit the axial strain in the fiber direction of a ply. Using the limit of fiber strain as a criterion is in use at Northrop Grumman[4]. The wall thickness corresponds to one of the ply types reaching the strain limit. Before comparing the strains in the fiber direction, the strains in the x-s coordinate system have to be determined first. The inversion of Eq. (1) shows the expressions for them.

$$\begin{Bmatrix} \varepsilon_{xx} \\ \gamma_{xs} \end{Bmatrix} = \frac{1}{(1-\beta_1^2)} \begin{bmatrix} \frac{1}{K_{11}} & -\frac{K_{12}}{K_{11}K_{22}} \\ -\frac{K_{12}}{K_{11}K_{22}} & \frac{1}{K_{22}} \end{bmatrix} \begin{Bmatrix} N_{xx} \\ N_{xs} \end{Bmatrix} \tag{12}$$

Then the strain transformation equations are used to determine fiber direction strains for all ply types. The strain for each ply type with a rotation angle θ with respect to the x-s coordinate system is

$$\varepsilon = \frac{1}{h(1-\beta_1^2)} \left[\left(\frac{a_{12}}{k_{11}} - \frac{a_{26}\beta_1^2}{k_{12}} \right) N_{xx} + \left(\frac{a_{26}}{k_{22}} - \frac{a_{12}\beta_1^2}{k_{12}} \right) N_{xs} \right] \tag{13}$$

where a_{12} and a_{26} are defined as follows

$$a_{12} = \cos^2\theta - \sin^2\theta \left(\frac{A_{12}}{A_{22}} \right) \tag{14}$$

$$a_{26} = \sin\theta\cos\theta - \sin^2\theta \left(\frac{A_{26}}{A_{22}} \right) \tag{15}$$

The cover wall thickness is determined by comparing the strains for all the ply types in the configuration and determine when the limit is reached first. The steps in this analysis are indicated in Fig. 6.

Design Analysis Methodology for Laminate Rotation

The stress resultants in the x-s coordinate system are transformed to the x_ψ-y_ψ coordinate system with an angle ψ in order to get the strain-stress resultant relationship.

$$\begin{Bmatrix} \varepsilon_{x\psi} \\ \varepsilon_{y\psi} \\ \gamma_{12} \end{Bmatrix} = [A]^{-1} \begin{Bmatrix} N_{x\psi} \\ N_{y\psi} \\ N_{xy\psi} \end{Bmatrix} \tag{16}$$

where $[A]^{-1}$ is the inverse of the A matrix.

. Using the same design criterion as Angle Ply Rotation, the wall thickness also corresponds to one of the ply types reaching the strain limit. The strain in the fiber directions can be found by using strain transformation equations. They are known by transforming the strains in the x_ψ-y_ψ coordinate system to 0° for axial plies, θ for balanced angle plies and 90° for transverse plies. The steps in this analysis are shown in Fig. 7.

Deformation Parameters

After the wall thickness has been found for the appropriate design strategy, the behavior of the structure can be determined. For only torsion and spanwise bending, the governing equations are

$$M_x = C_{44}\phi_{,x} + C_{45}(-W_{,xx}) \tag{17}$$

$$M_y = C_{45}\phi_{,x} + C_{55}(-W_{,xx}) \tag{18}$$

Eqs. (17) and (18) relate the moments to the rate of twist, $\phi_{,x}$, and bending curvature, $W_{,xx}$, of the structure. The moments in the x and y directions are M_x=2CsHN_{xs}, nose up moment, and M_y=-N_{xx}CsH, spanwise lift (Fig. 3). The rate of twist and bending curvature of the structure can be determined from Eqs. (17) and (18) by inversion.

$$\phi_{,x} = \frac{1}{C_{44}C_{55}\left(1-\beta^2\right)}\left(C_{55}M_x - C_{45}M_y\right) \tag{19}$$

$$W_{,xx} = \frac{1}{C_{44}C_{55}\left(1-\beta^2\right)}\left(C_{45}M_x - C_{44}M_y\right) \tag{20}$$

Camber curvature is estimated by the following equations[7]:

$$\kappa_c = \frac{2}{H}\left(\bar{C}_{12}\varepsilon + \bar{C}_{26}\frac{N_{xs}}{K_{22}}\right) \tag{21}$$

where $\bar{C}_{12}$ is an effective Poisson's ratio

$$\bar{C}_{12} = \frac{A_{12}}{A_{22}} - \frac{A_{26}}{A_{22}}\frac{K_{12}}{K_{22}} \tag{22}$$

and $\bar{C}_{26}$ characterizes the coupling between twist and camber

$$\bar{C}_{26} = \frac{A_{26}}{A_{22}} \tag{23}$$

This completes the analysis for each configuration. Note that no special effort has been made to tailor for camber response. The focus has been only on bend-twist coupling.

TRANSPORT ILLUSTRATION

A specific transport illustration is created for analysis using the two design strategies. The model shown in Figure 3 with the dimensions of the C-130 aircraft center wing box (Fig. 8) is used. The material system for the simple box model is AS4/3501-6 carbon-epoxy. Its elastic properties are shown in Table 1. The stress resultants in the covers are assumed to be 25,000 pounds per inch for N_{xx}, and 5,000 pounds per inch for N_{xs}. The limit for the axial strain in the fiber direction of a ply is set to be 4500

microstrain. The configuration for the Angle Ply Rotation design strategy is 50% of axial plies and 50% of angle plies; the configuration for the Laminate Rotation design strategy is 50% of axial plies and 50% of [±45]. These 50-50 configurations are simplified approximations to the wings of the F-18 and the AV-8B aircraft. The transverse plies are neglected for both design strategies for simplicity. The webs are fixed at [±45], which is based on the unanimous recommendations of Refs. 4-6. For simplicity, the thicknesses for the front spar web and the rear spar web are chosen to be the same. The web wall thickness is chosen to be forty percent of the cover thickness. The analysis is based on this specific wing section and loads. Results are presented for designs using Laminate Rotation in Figs. 9-13 and Angle Ply Rotation in Figs. 14-18.

RESULTS AND DISCUSSION

Preliminary Remarks

The illustration corresponds to a transport aircraft wing section, which is that of the center wing of the C-130. Thus, the results presented strictly correspond to this configuration. This geometry, the chosen material system, design criterion adopted, loading considered and strategies used, all contribute to the analytical results and the discussion of them. The intention has been to provide an overall, unique assessment of wing sections with bend-twist coupling. Additional parametric studies and further research are needed to determine if the trends are general.

Laminate Rotation

The angle ψ corresponds to the rotation of the laminate with respect to the axis of the structure.

The following observations are based upon the results in Figs. 9-13. The observations are:

1. The thickness curves have the same geometric shape as the bending and torsional stiffness curves with identically placed cusps (Fig. 9 and 10).
2. The cusps correspond to distinct transitions between ply types reaching the design strain limit. If the design limit were raised for the same material system, the thickness curve would be lowered, but would maintain the same shape.
3. If the ratio between N_{xx} and N_{xs} is nearly constant, but with absolute values reduced, the thickness curve would be lowered as above.
4. Changing the mix of plies would likely alter the cusp points, but not the general shape of the curves.
5. Due to cusp placement, the curve of C_{45} is not exactly skew symmetric (Fig. 10).
6. The rate of twist and bending curvature curves have the same cusp points but opposite curvature for the thickness curve. As a higher thickness corresponds to greater stiffness, these trends make physical sense (Fig. 11 and 12).
7. A different trend can be noticed at approximately –60 and –30 degrees in Figs.11 and 12, respectively. In the neighborhood of –60 degrees, the rate of twist is extremely low. In contrast, the bending curvature reaches a minimum near –30 degrees.
8. If it is desired to stabilize aeroelastically produced lift due to tailoring, the –60 degrees is a good choice for Laminate Rotation, since it tends to reduce section stall and increase resistance to torsional divergence.

9. The camber curvature is small, and it does not follow similar trends to the other parameters. Recall that no effort has been made to design for camber (Fig. 13).
10. More bend-twist coupling does not necessarily correspond to the coupled global stiffnesses, as shown in Figs. 11-13.

Angle Ply Rotation

The following observations are based upon the results in Figs. 14-20. Due to different configurations of ply layups, the results for Angle Ply Rotation cannot be directly compared to the results for Laminate Rotation. The angle θ is the angle ply orientation with respect to a fixed [0] axis. The following observations are made:

1. There is one less cusp to the curves for thickness, stiffness, rate of twist and bending curvature. There is a cusp at $\theta=0°$, which could be evaluated by a separate analysis. The way the current program is written as shown in Appendix A, $\theta=0°$ corresponds to dividing by zero, which cannot be determined.
2. Even though the two design strategies cannot be compared directly, there are still some noticeable differences between them. From Fig. 19, the thickness for Angle Ply Rotation that is required to satisfy the design requirements is less than thickness for Laminate Rotation.
3. There is less bend-twist coupling and greater twisting stiffness for negative ply rotation (Fig. 15). The bending stiffness is greater for negative angle ply rotation, θ, than for negative laminate rotation, ψ. The curves are affected by the cusps.
4. Compared to Laminate Rotation, the coupled bending stiffness for Angle Ply Rotation is increased and the coupled torsional stiffness is decreased. Based on

the changes in stiffnesses, the value of the rate of twist for Angle Ply Rotation is greater than Laminate Rotation.

5. Not only the rate of twist has been affected; the global compliance of bending curvature for Angle Ply Rotation is less than Laminate Rotation.
6. The camber curvature is greater for Angle Ply Rotation than Laminate Rotation for positive rotation, but the reverse is true for negative rotations (Fig. 20).

Concluding Remarks

An aircraft illustration of the two design strategies has been presented. The trends are likely to be affected by selected loading magnitudes and their respective ratios, which may be altered by control surfaces and internal features of the structure such as ribs.

SUMMARY

In this study, two design strategies specifically chosen to produce spanwise bend-twist coupling have been presented and illustrated. The illustration that has been chosen is the center wing section of a transport wing. Even though the results of the two design strategies show some similarities, the wing cover ply layups are so different that they cannot be directly compared. It does appear, however, that the new angle ply rotation strategy may produce a lighter weight structure.

This study is only a beginning. In order to understand these two design strategies well, much future work is needed.

REFERENCES

1. Rehfield, L.W., "Design Analysis Methodology for Composite Rotor Blades," Proceedings of the Seventh DoD/NASA Conference on Fibrous Composites in Structural Design, Denver, Colorado, June 17-20 1985, AFWAL-TR-85-3094, pp. (V(a)-1)-(V(a)-15).

2. Shirk, M.H., Hertz, T.J., Weisshaar, T.A., "Aeroelastic Tailoring – Theory, Practice, and Promise," Journal of Aircraft, Vol. 23, No.1, January 1986, pp. 6-17.

3. Rehfield, L.W., "A Refined Simple Model for Tailoring Box Beams with Composites," Proceedings of the 42nd AIAA/ASME/ASCE/AHS/ASC Structures, Structural Dynamics, and Materials Conference and Exhibit, AIAA, Seattle, Washington, April 16-19, 2001, AIAA paper 2001-1333, published on CD ROM, AIAA, Reston, VA, 2001.

4. Private Communication, Mahler, M., Northrop Grumman Corporation, El Segundo, CA, 2002.

5. Private Communication, Garrett, R.A., McDonnell Aircraft Company (Retired), St. Louis, MD, 2002.

6. Private Communication, Renton, W.J., Boeing Phantom Works, Kent, WA, 2002.

7. Rehfield, L.W., Chang, S., Zischka, P.J., "Modeling and Analysis Methodology for Aeroelastically Tailored Chordwise Deformable Wings," NASA Contractor Report 189620, Contract NAS1-18754, July 1992.

TABLE 1. NOMINAL UNIDIRECTIONAL MECHANICAL PROPERTIES FOR AS4/3501-6 GRAPHITE-EPOXY (ROOM TEMPERATURE, DRY)

FIBER DIRECTION, TENSION MODULUS, E_{11}	20.0×10^6 psi
TRANSVERSE DIRECTION, TENSION MODULUS, E_{22}	1.7×10^6 psi
IN-PLANE SHEAR MODULUS, G_{12}	0.85×10^6 psi
POISSONS'S RATIO, ν_{12}	0.30

FIGURE 1 – ANGLE PLY ROTATION

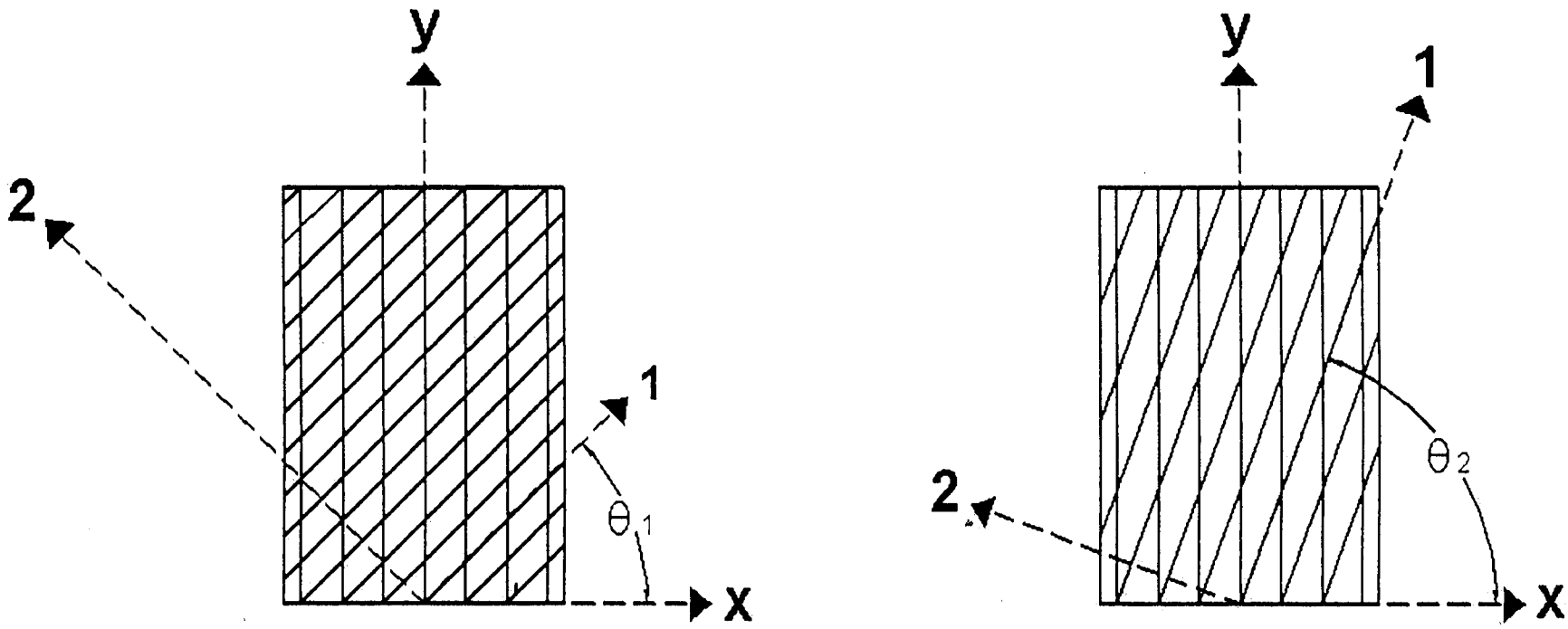

FIGURE 2 – LAMINATE ROTATION

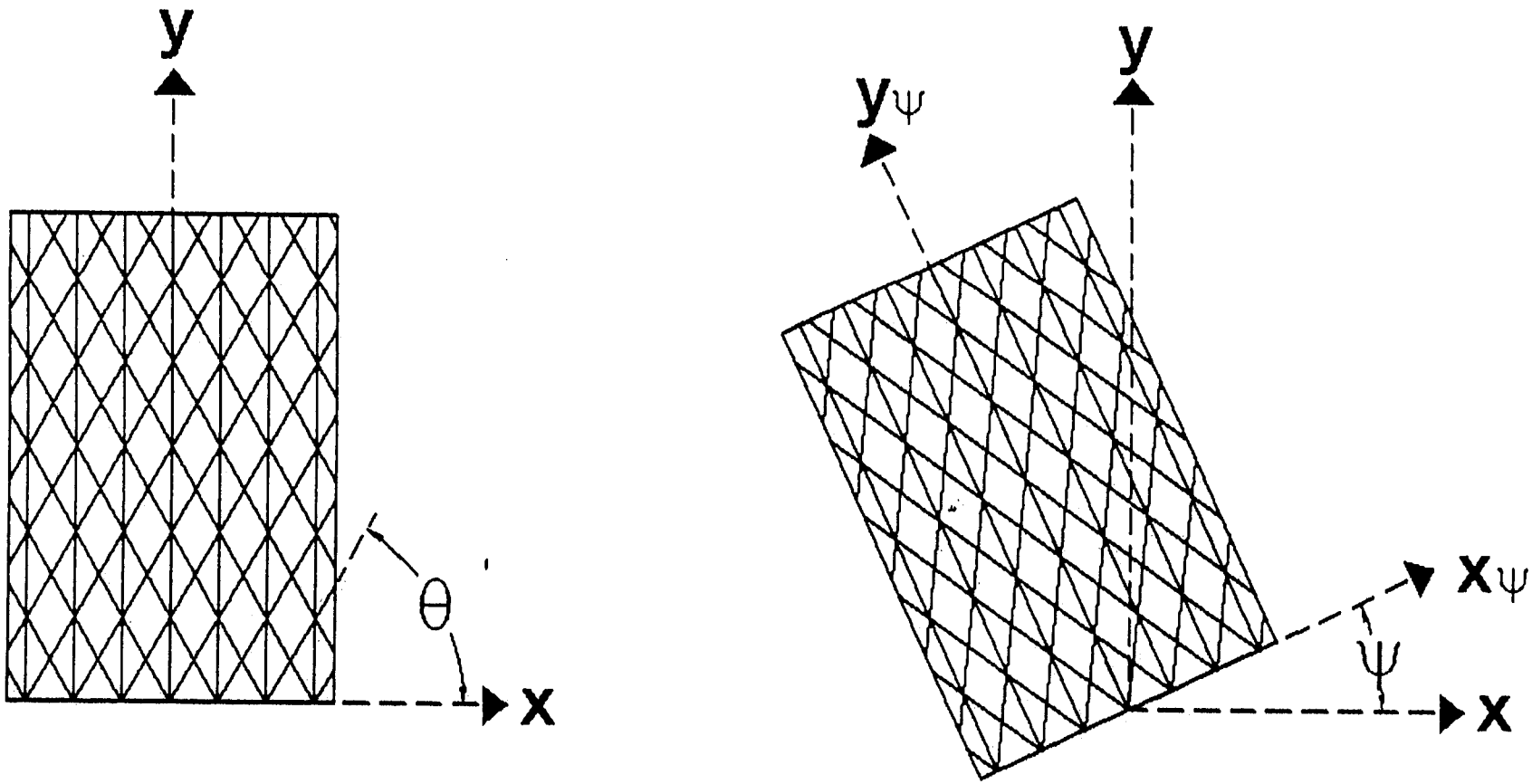

FIGURE 3 – BOX MODEL WITH WEBS MODELED

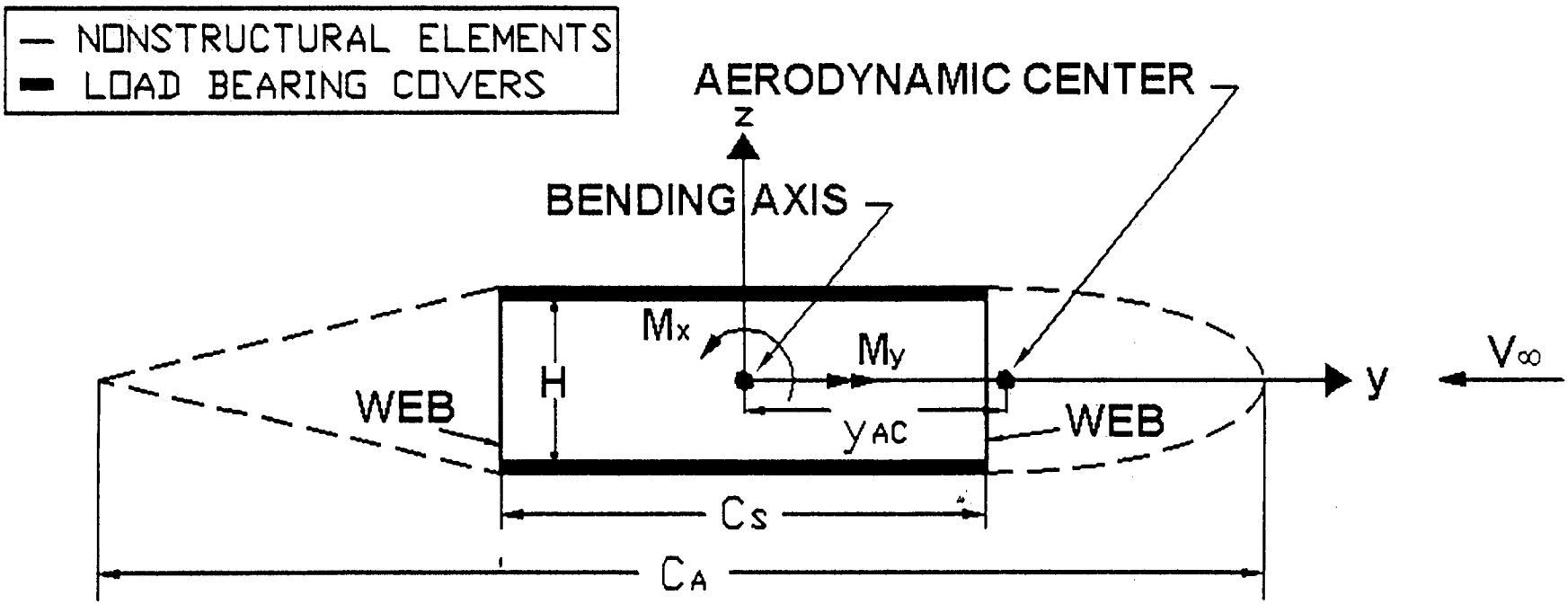

FIGURE 4 – SIGN CONVENTION FOR PLY ORIENTATION AND LAYUP

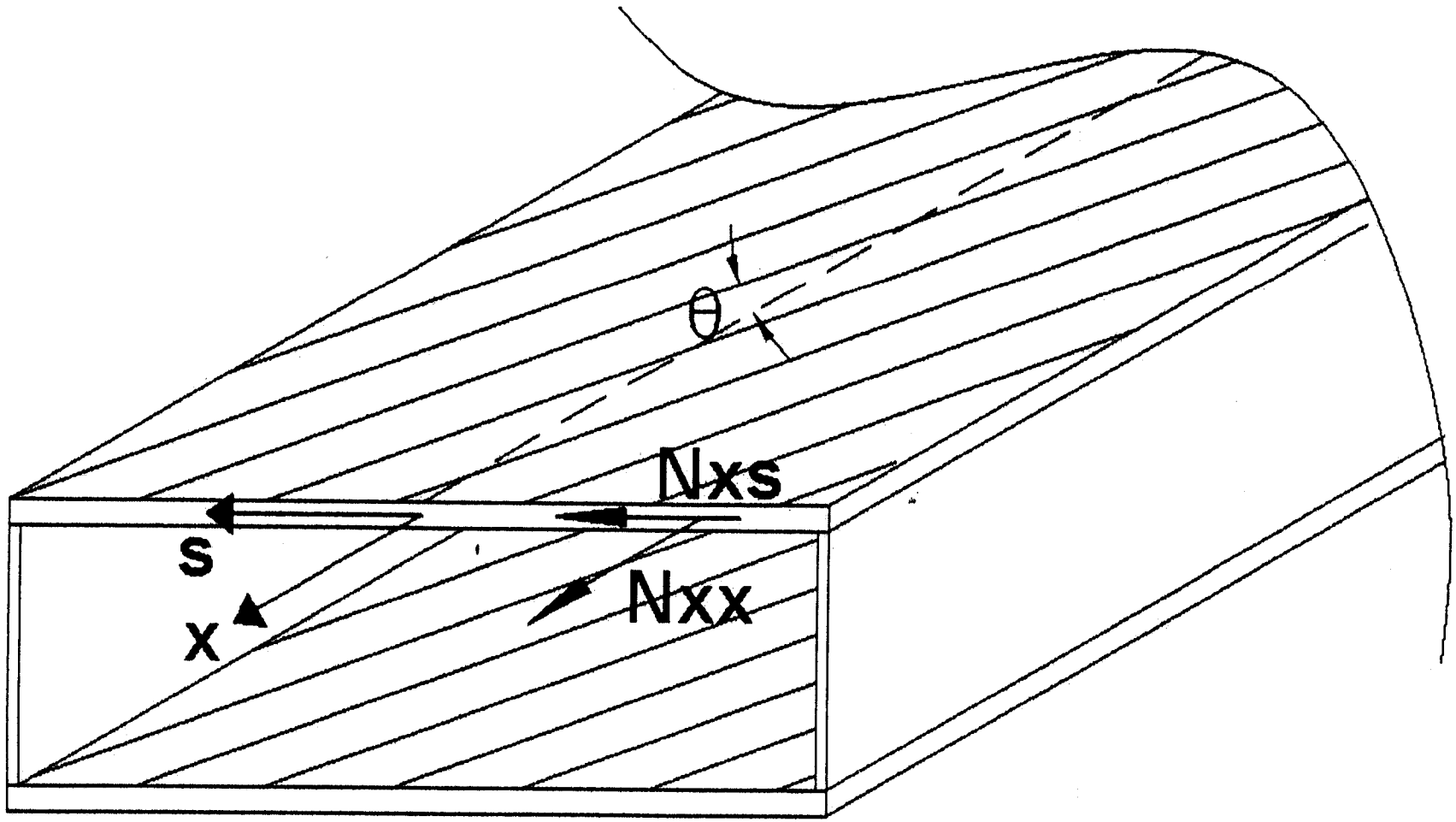

FIGURE 5 – PLY ORIENTATION FOR THE COVERS

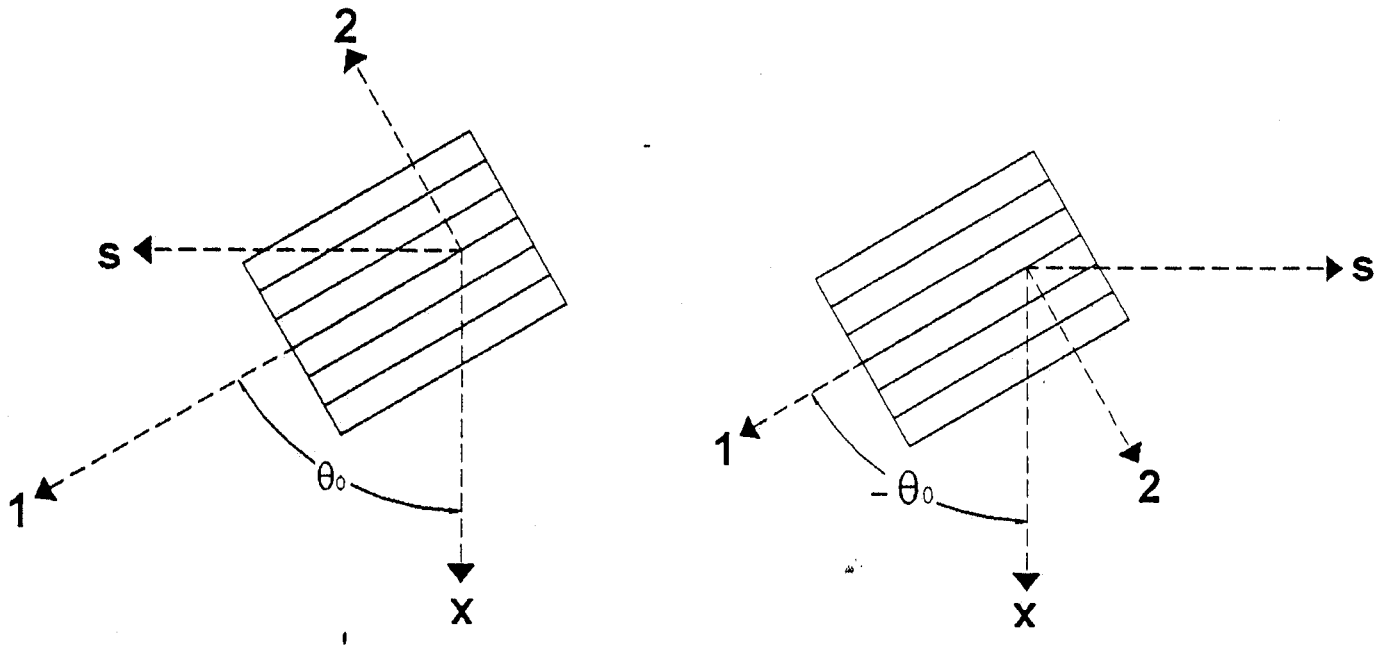

Upper Cover

Lower Cover

FIGURE 6 – FLOW DIAGRAM FOR DESIGN ANALYSIS METHODOLOGY FOR ANGLE PLY ROTATION

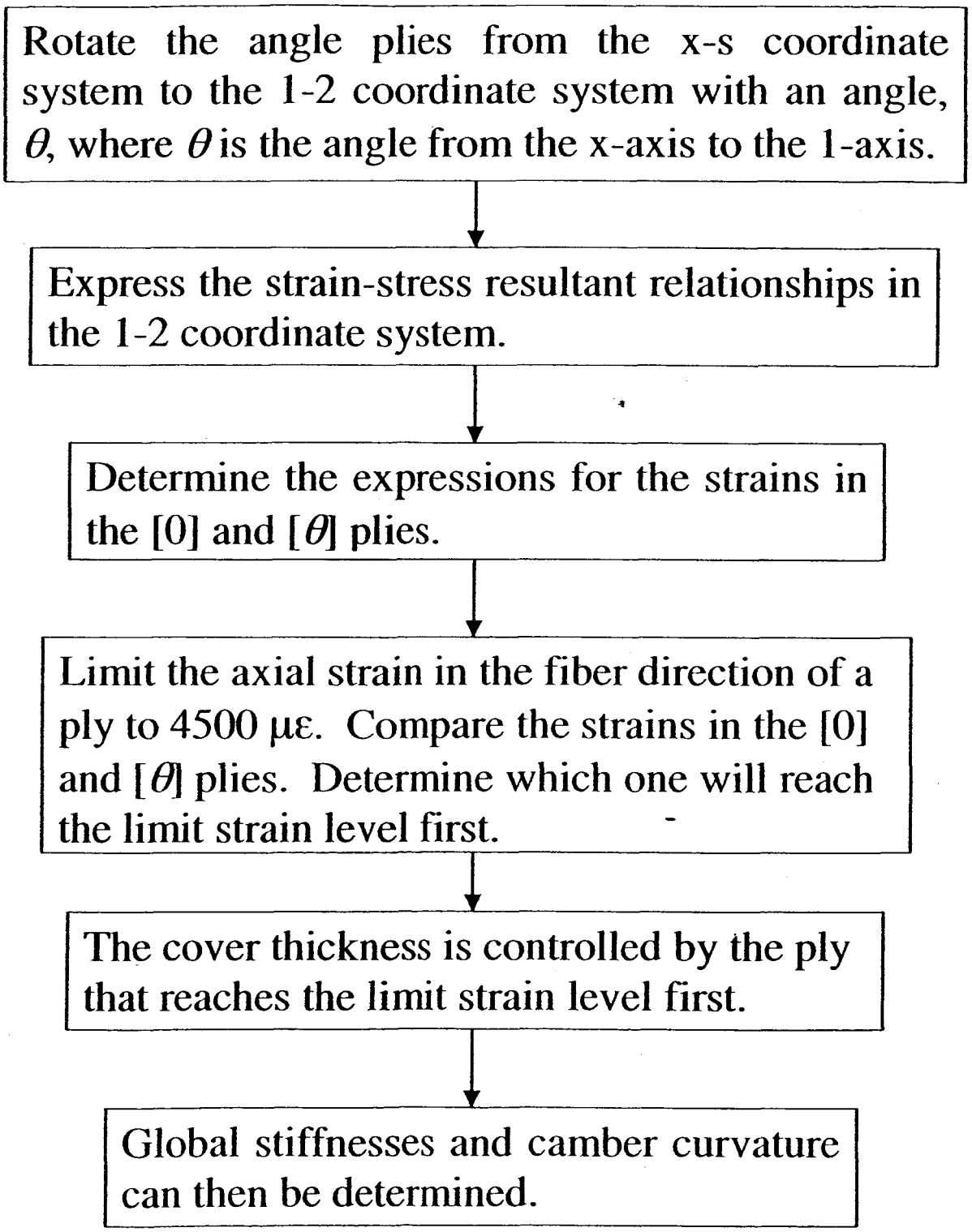

FIGURE 7 – FLOW DIAGRAM FOR DESIGN ANALYSIS METHODOLOGY FOR LAMINATE ROTATION

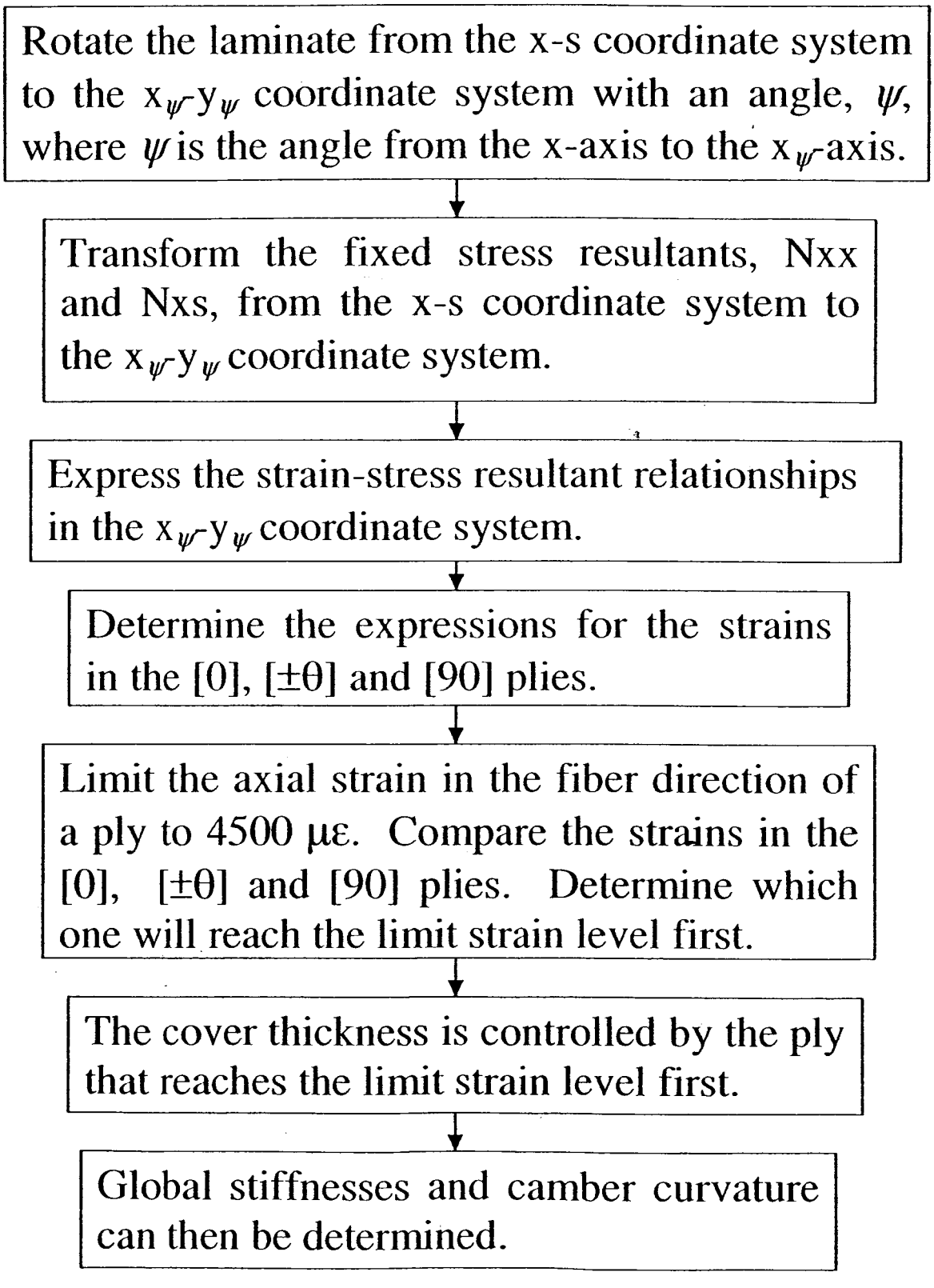

FIGURE 8 – C-130 BOX DIMENSIONS

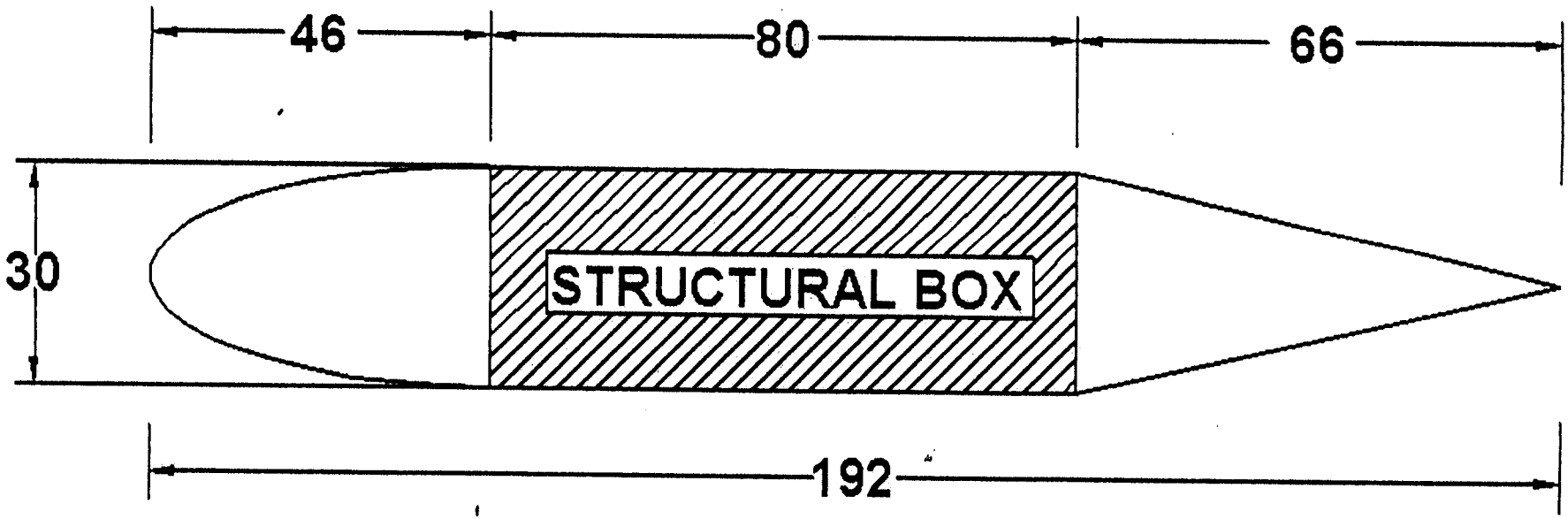

NOTE: ALL UNITS ARE IN INCHES

FIGURE 9 THICKNESS VS. LAMINATE ROTATION
for (50% [0], 50% [±45], 0.4 web's thickness)

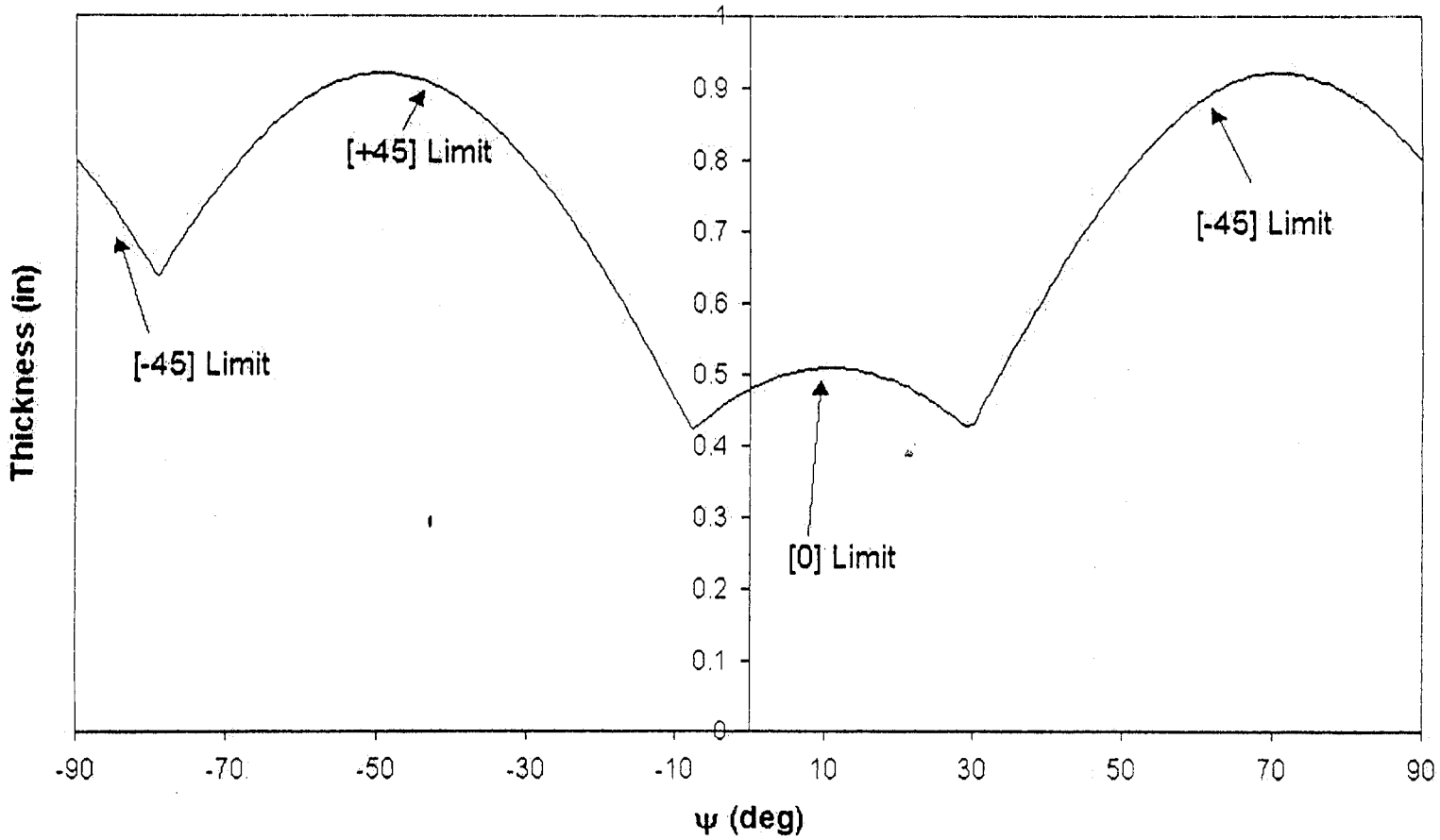

FIGURE 10 STIFFNESSES VS. LAMINATE ROTATION
for (50% [0], 50% [±45], 0.4 web's thickness)

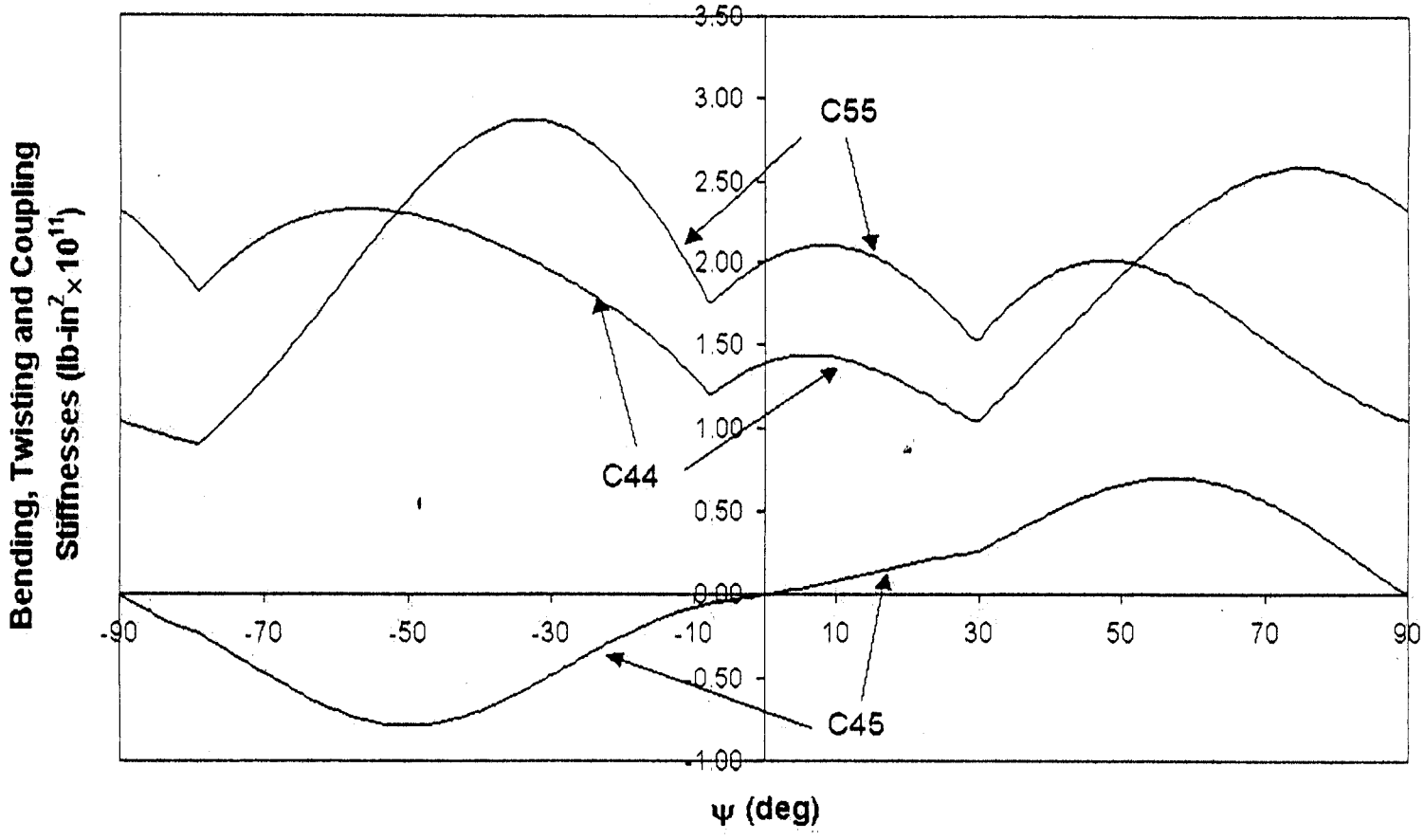

FIGURE 11 RATE OF TWIST VS. LAMINATE ROTATION
for (50% [0], 50% [±45], 0.4 web's thickness)

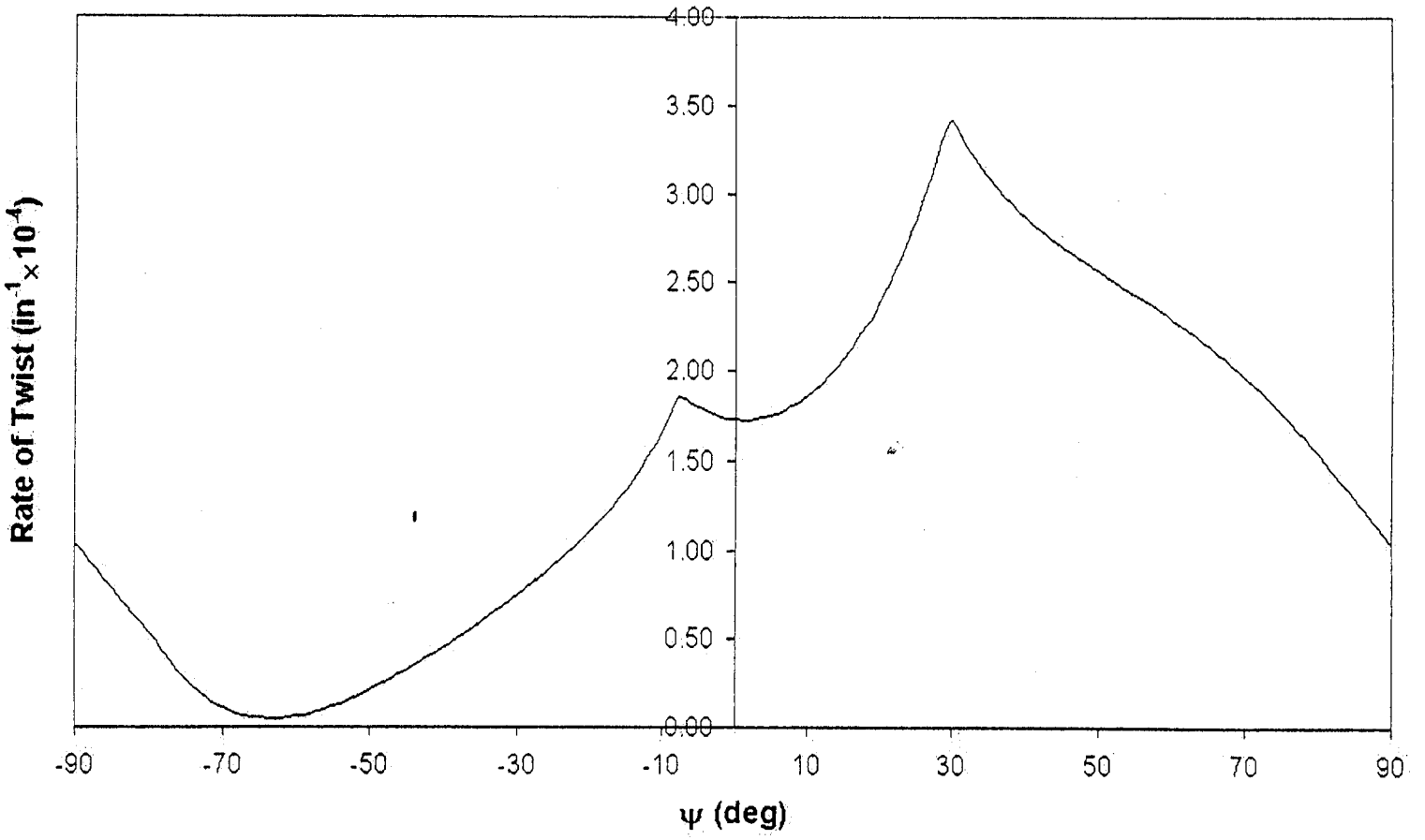

FIGURE 12 BENDING CURVATURE VS. LAMINATE ROTATION
for (50% [0], 50% [±45], 0.4 web's thickness)

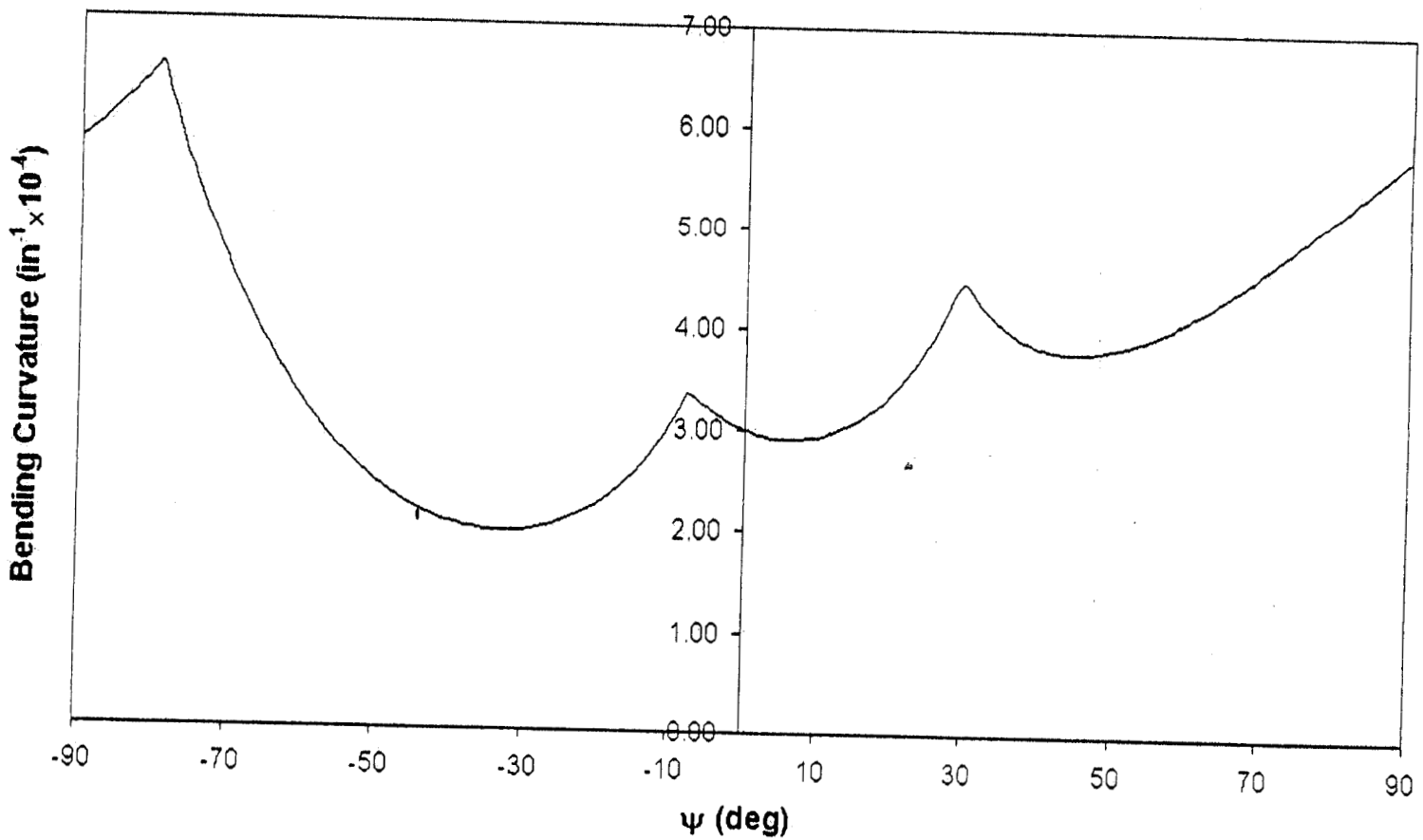

FIGURE 13 CAMBER CURVATURE VS. LAMINATE ROTATION
for (50%[0], 50% [±45], 0.4 web's thickness)

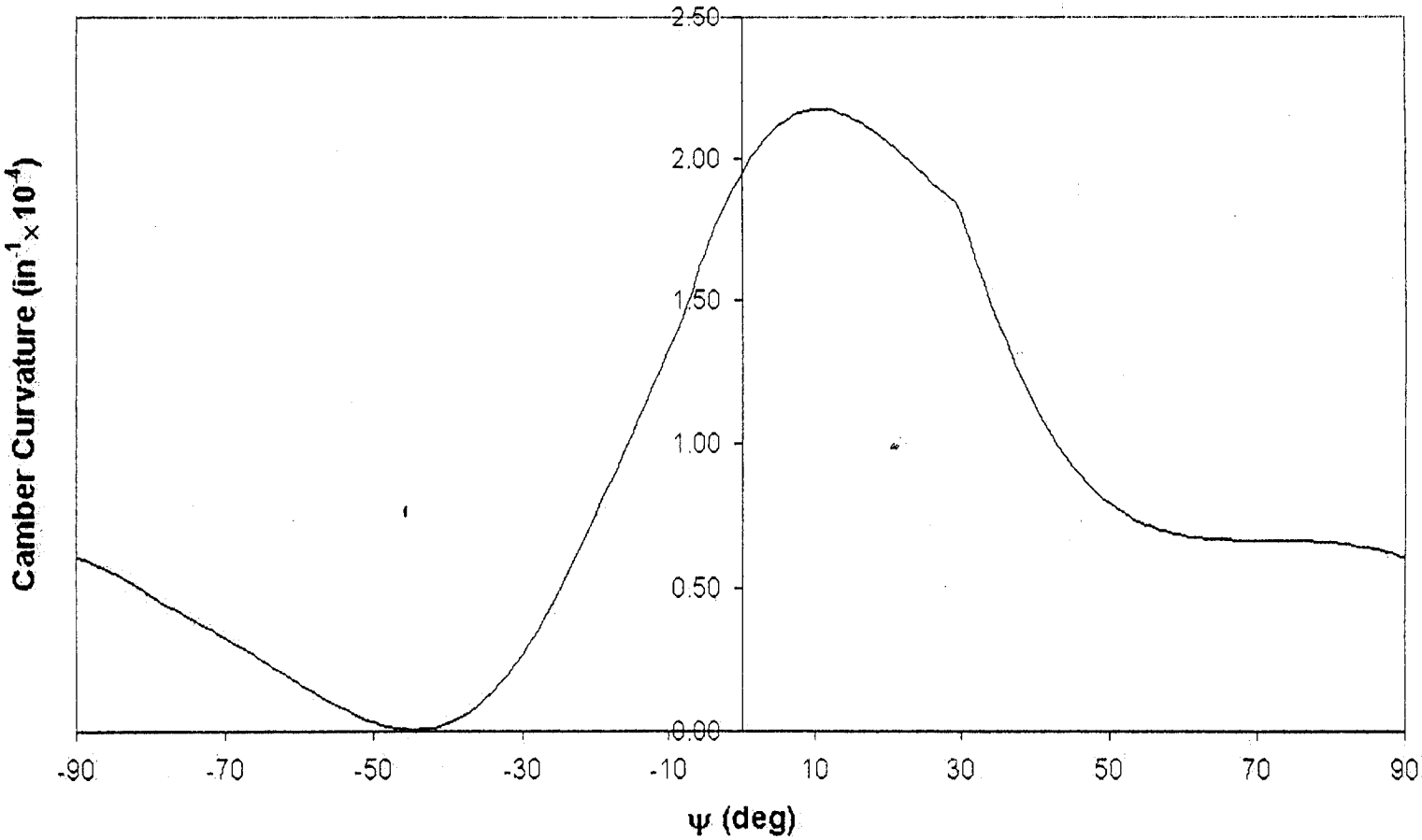

FIGURE 14 THICKNESS VS. ANGLE PLY LAYUP ORIENTATION
for (50% [0], 50% [θ], 0.4 web's thickness)

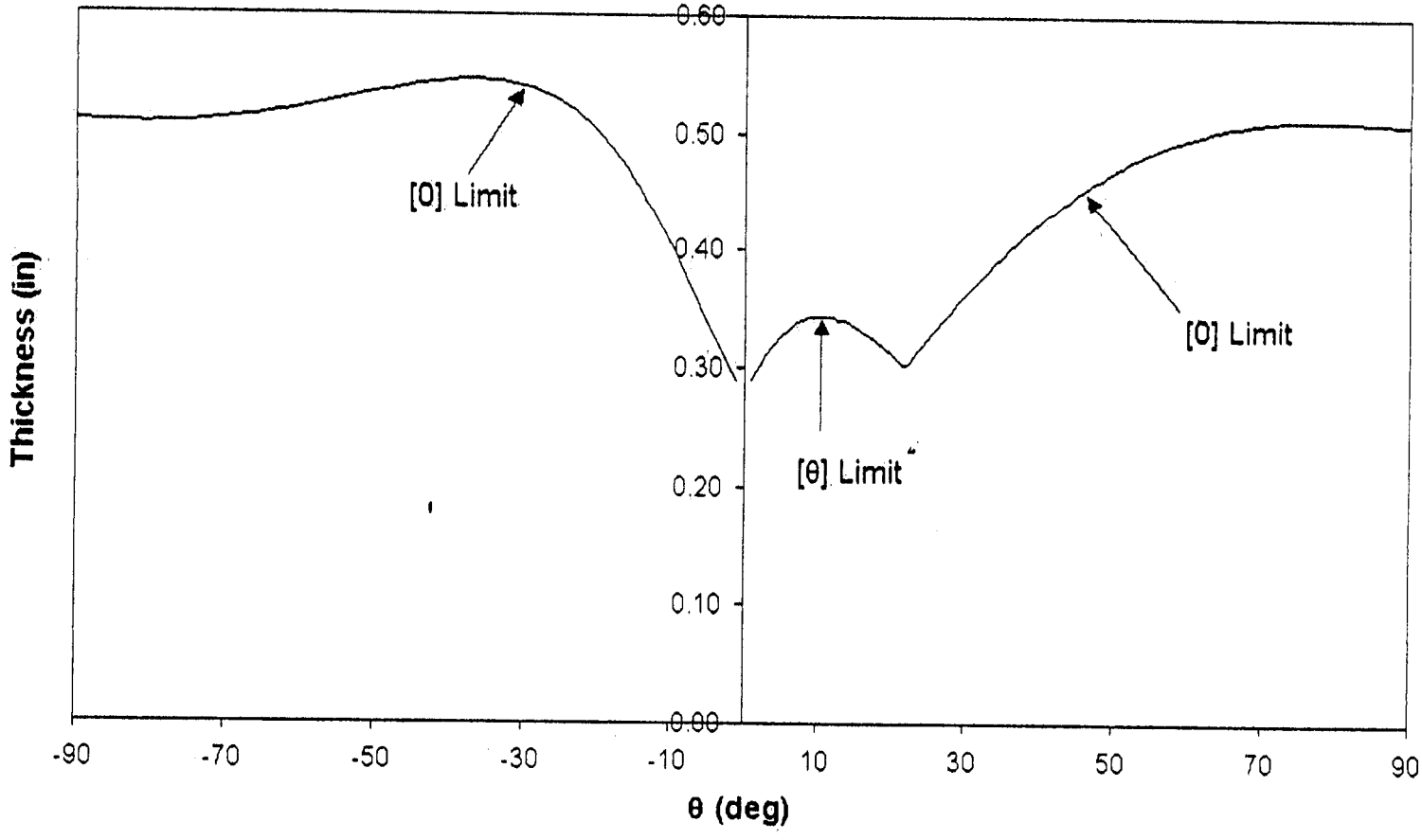

FIGURE 15 BENDING, TWISTING and COUPLING STIFFNESSES VS. ANGLE PLY LAYUP ORIENTATION
for (50% [0], 50% [θ], 0.4 web's thickness)

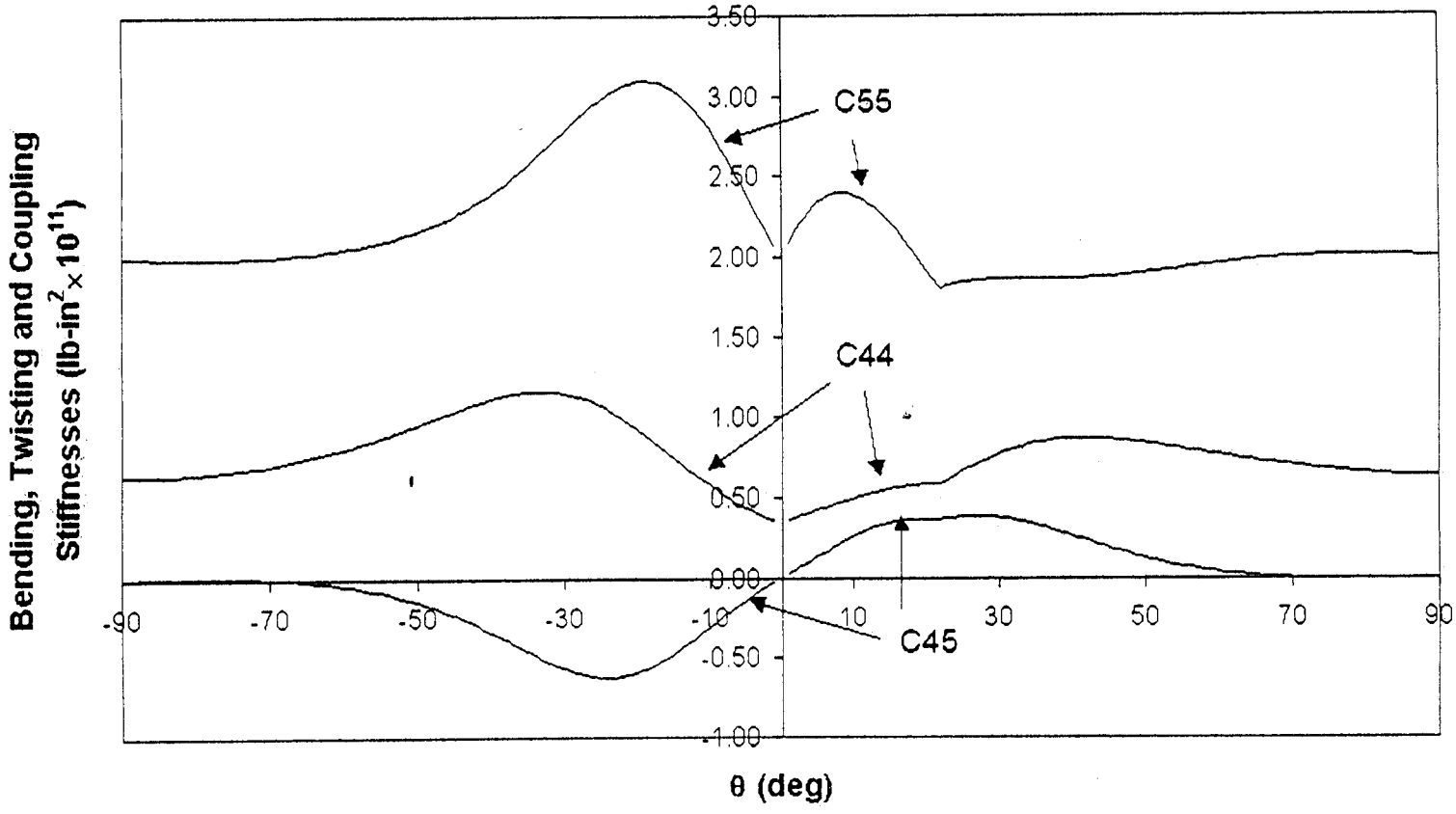

FIGURE 16 RATE OF TWIST VS. ANGLE PLY LAYUP ORIENTATION
for (50% [0], 50% [θ], 0.4 web's thickness)

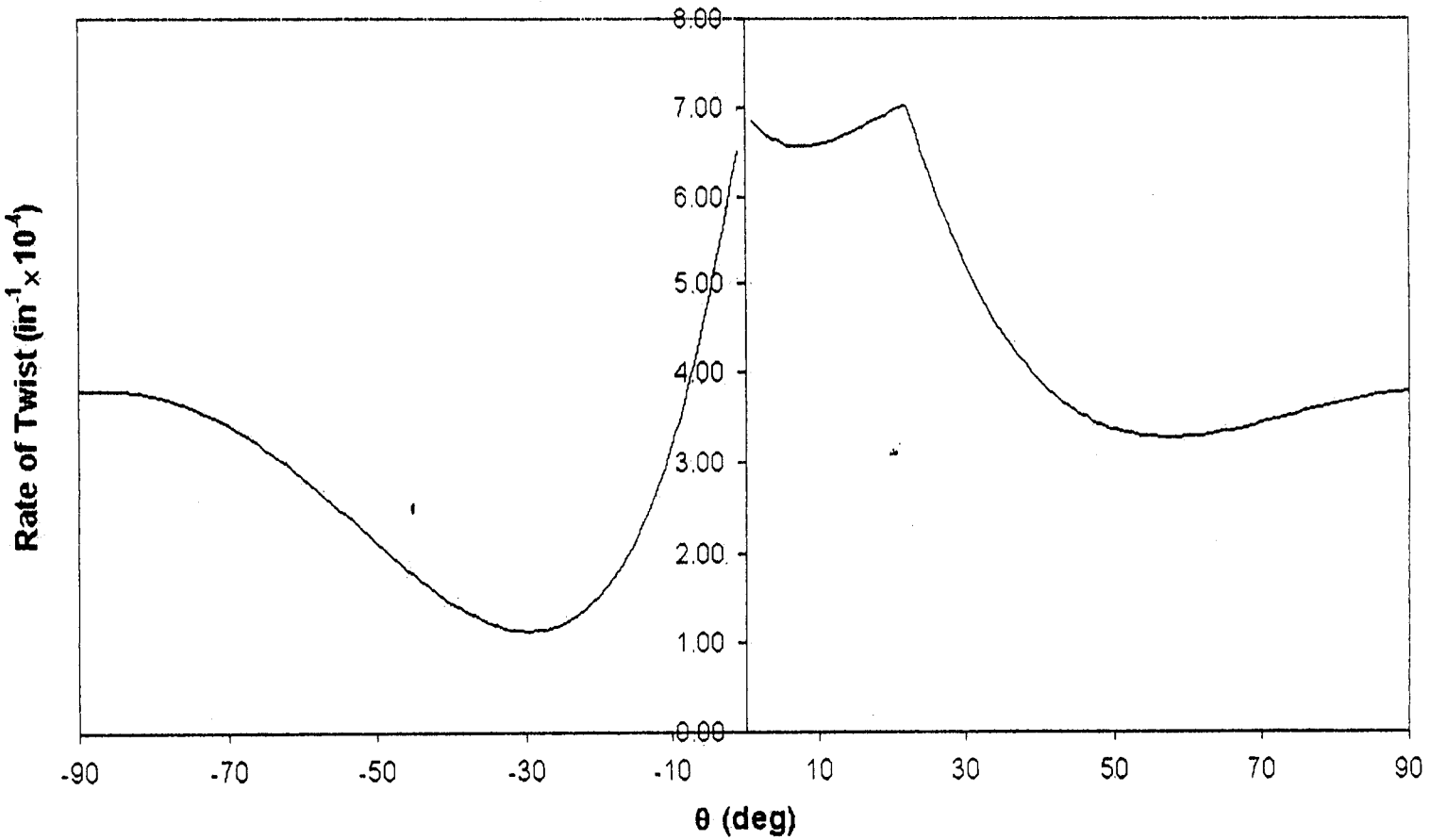

FIGURE 17 BENDING CURVATURE VS. ANGLE PLY LAYUP ORIENTATION
for (50% [0], 50% [θ], 0.4 web's thickness)

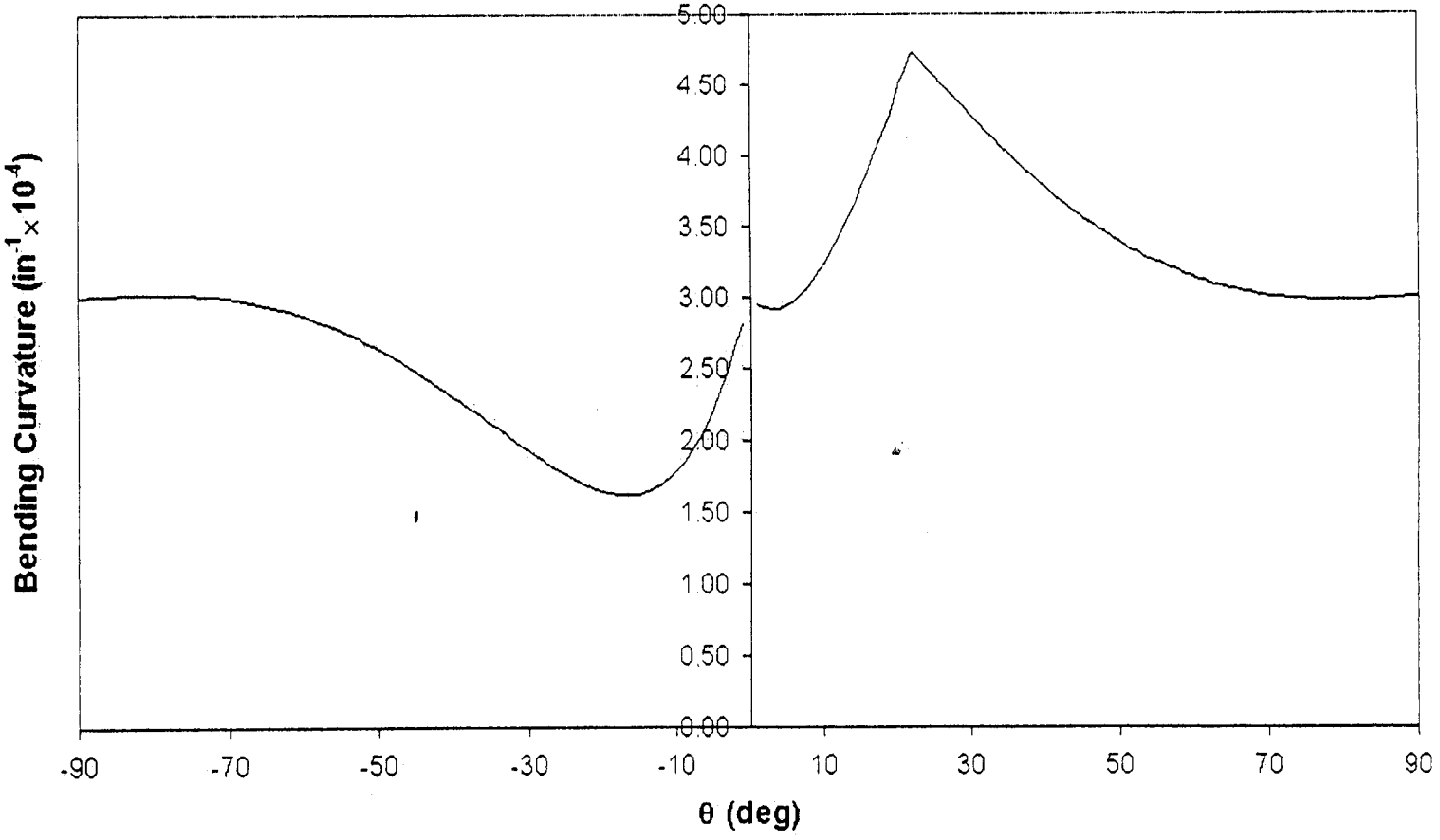

FIGURE 18 CAMBER CURVATURE VS. ANGLE PLY LAYUP ORIENTATION
for (50% [0], 50% [θ], 0.4 web's thickness)

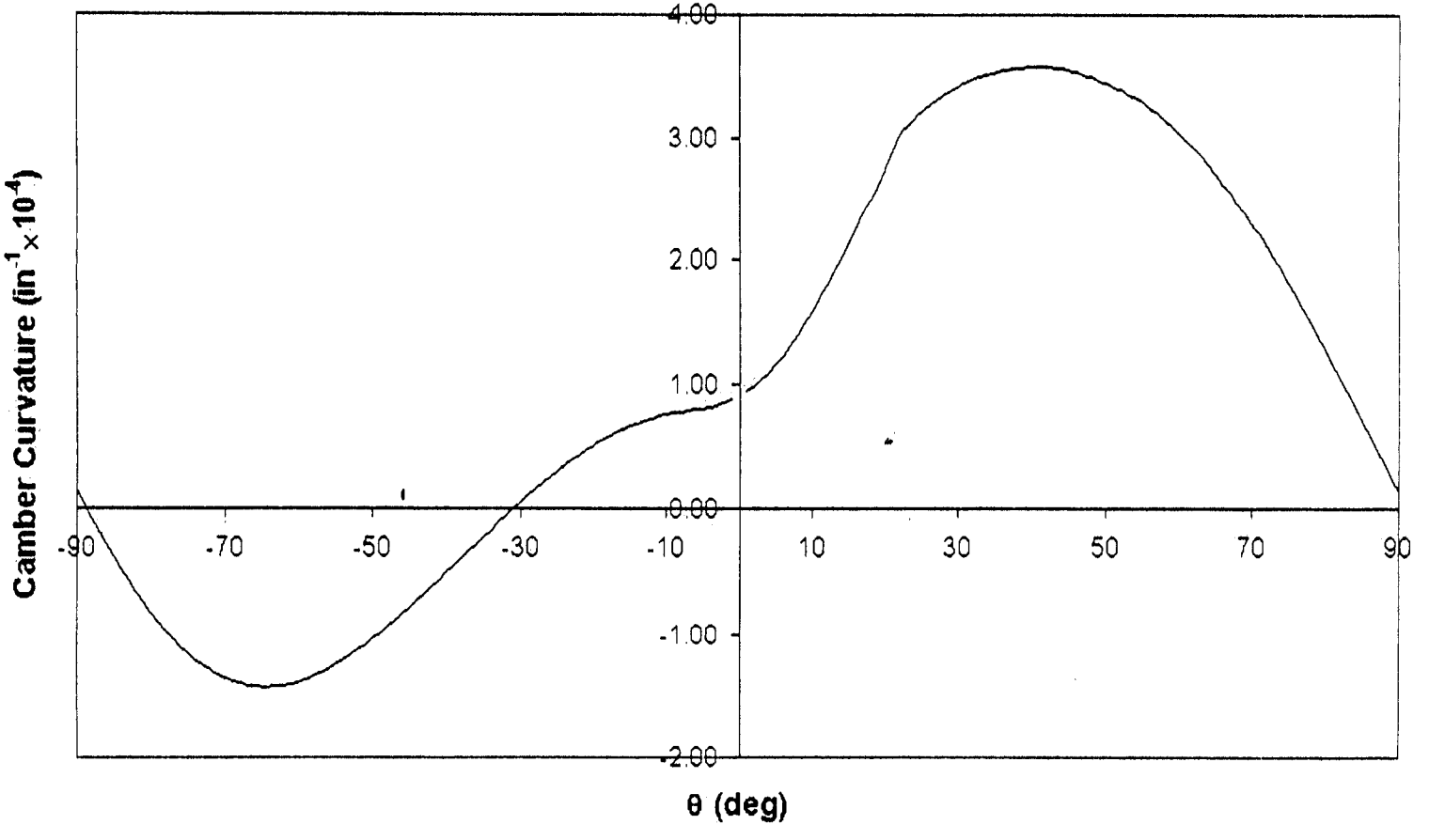

FIGURE 19 COMPARATIVE THICKNESS
for (50% [0], 50% [θ], 0.4 web's thickness)

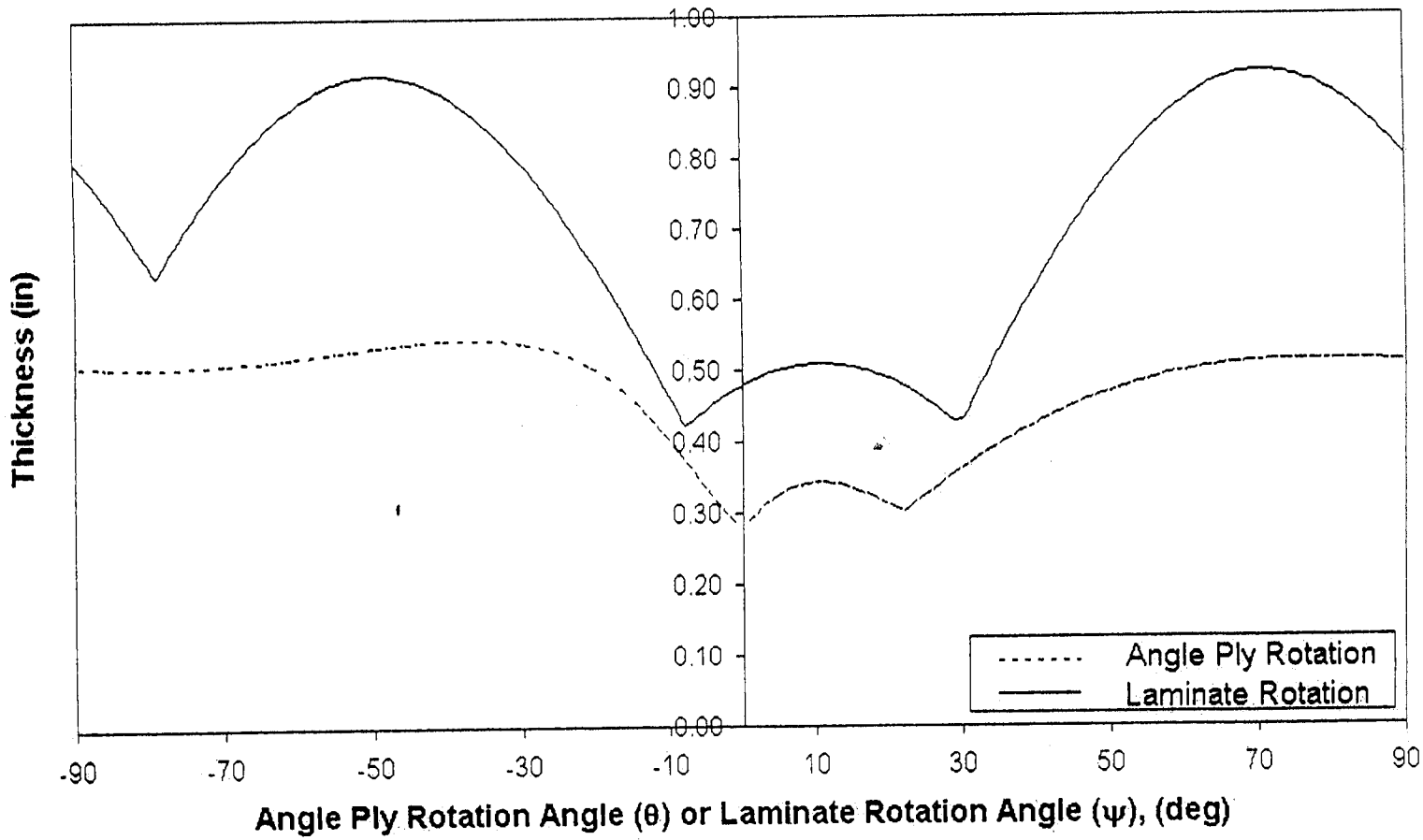

FIGURE 20 COMPARATIVE CAMBER CURVATURE
for (50% [0], 50% [θ], 0.4 web's thickness)

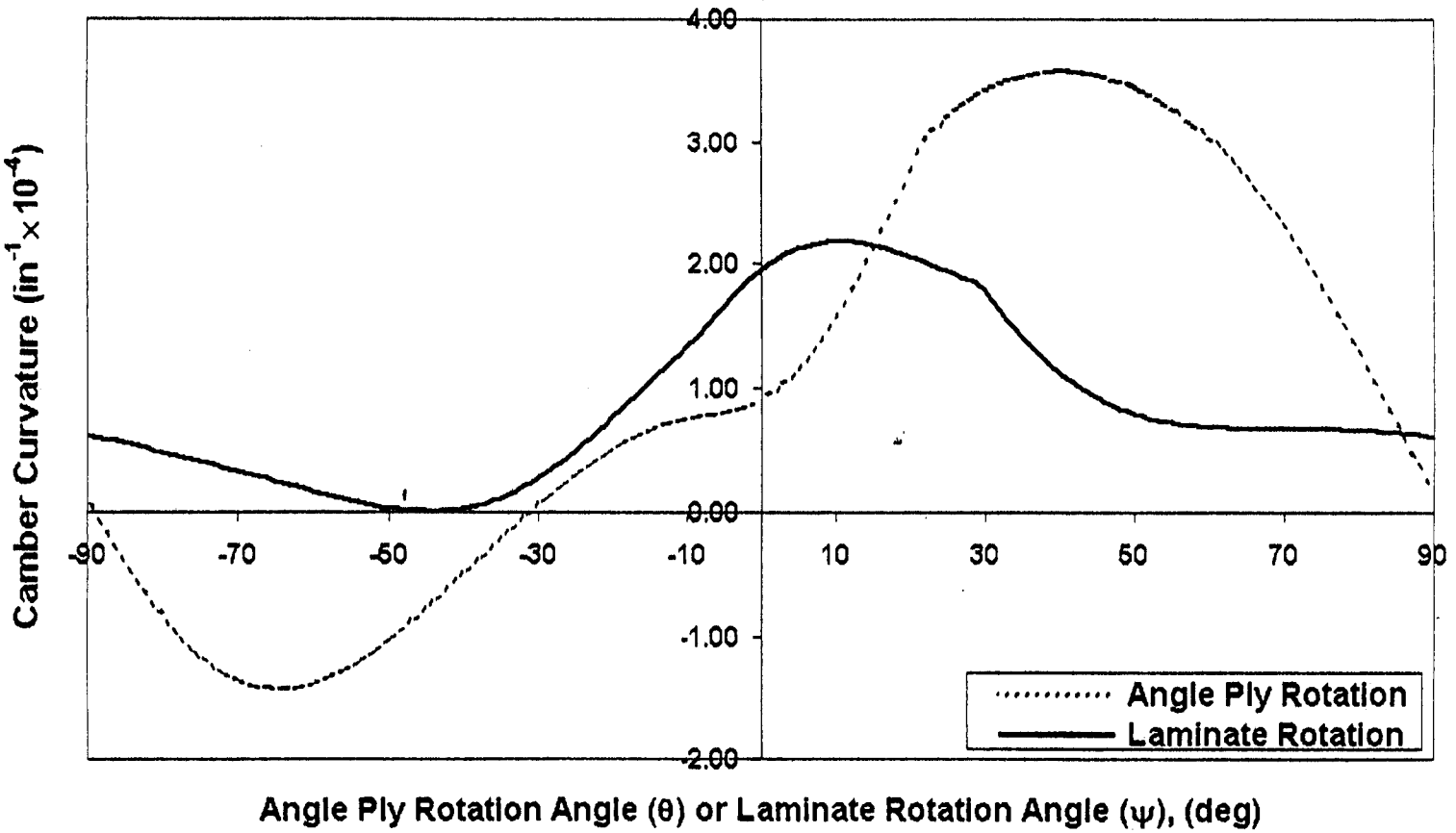

APPENDIX A

PROGRAM FOR ANGLE PLY ROTATION

Variable and Parameter Definitions

Appendix A is the Fortran 90 program that is used to analyze Angle Ply Rotation.

The following inputs are required for the program.

Inputs:

Width of the box model, Cs
Height of the box model, H
Elastic properties of the materials used for the box model, E_{11}, E_{22} and G_{12}
Limit strain for the design criterion, ε
Axial loading due to bending, N_{xx}, and due to torsion, N_{xs}
Configuration of the ply layup – fractions of axial plies, angle plies and transverse plies, which are f_0, f_θ, f_{90}.
Orientation for the ply layup of the webs, w
Fraction of the wall thickness for the front spar web, ff
Fraction of the wall thickness for the rear spar web, fr

After inputting the values for the above parameters, the program generates the following outputs.

Outputs:

Bend-twist coupling parameter, β^2
Thickness of the covers, h
Rate of twist, $\phi_{,x}$
Bending curvature, $W_{,xx}$
Camber curvature, kc
Global stiffnesses, C_{44}, C_{55}, and C_{45}
Relative weight, which is compared to a balanced brenchmark reference of [0] and [45] plies.

Notes: All of the inputs are in degrees and English units.

Program Listing

```
c==============================
c PROGRAM for Angle Ply Rotation
c==============================
      Program coupling
   real*8 E11,E22,G12,v12,v21,Q11,Q12,Q22,Q66,C44,C45,C55
```

```
      real*8 Qbar11u,Qbar12u,Qbar22u,Qbar16u,Qbar26u,Qbar66u,eps
          real*8 Qbar11l,Qbar12l,Qbar22l,Qbar16l,Qbar26l,Qbar66l
          real*8 Qbar11w,Qbar12w,Qbar22w,Qbar16w,Qbar26w,Qbar66w
          real*8 Qbar11b,Qbar12b,Qbar22b,Qbar66b
      real*8 Qb110,Qb120,Qb220,Qb160,Qb260,Qb660
      real*8 Qb11u,Qb12u,Qb22u,Qb16u,Qb26u,Qb66u,Q(4)
      real*8 Qb119,Qb129,Qb229,Qb169,Qb269,Qb669
          real*8 Qb11l,Qb12l,Qb22l,Qb16l,Qb26l,Qb66l
          real*8 Qb11p,Qb12p,Qb22p,Qb16p,Qb26p,Qb66p
          real*8 Qb11n,Qb12n,Qb22n,Qb16n,Qb26n,Qb66n
          real*8 Qb115,Qb125,Qb225,Qb165,Qb265,Qb665,d,e,betamax
      real*8 k11u,k12u,k22u,theta,betasq,Cs,He,sumf,f0,ftheta,f90
          real*8 k11l,k12l,k22l,c12u,c26u,kcu,thick,thickb,wgain,thetamax
          real*8 k11w,k12w,k22w,k11b,k22b,beta1,hbb,htb,Mx,My,dphi
      real*8 theta1,pi,a,c,Nxx,Nxs,a12,a26,a12b,a26b,hb,ht,w,ffw,frw,Wxx
          integer i
c-------------------------------------
c create the data files for the results
c-------------------------------------
      open(unit=11,file='result.dat',status='unknown')
          open(unit=12,file='result1.dat',status='unknown')
          open(unit=13,file='result2.dat',status='unknown')
          open(unit=14,file='result3.dat',status='unknown')
          open(unit=15,file='result4.dat',status='unknown')
          open(unit=16,file='result5.dat',status='unknown')
      pi=3.14159
          betamax=0.0
      write(*,*) 'Enter the width for the single beam box in inches'
      read(*,*) Cs
      write(*,*) 'Enter its height in inches'
      read(*,*) He
      write(*,*) 'Enter the properties of the material'
      write(*,*) 'E11?'
      read(*,*) E11
      write(*,*) 'E22?'
      read(*,*) E22
      write(*,*) 'G12?'
      read(*,*) G12
      write(*,*) 'v12?'
      read(*,*) v12
          write(*,*) 'strain?'
          read(*,*) eps
          write(*,*) 'Enter the axial load Nxx'
          read(*,*) Nxx
      write(*,*) 'Enter the shear flow Nxs'
      read(*,*) Nxs
```

```
        write(*,*) 'Enter the degree for the angle plies of the webs'
        read(*,*) w
        write(*,*) 'Enter the fraction for the front spar web'
        read(*,*) ff
        write(*,*) 'Enter the fraction for the rear spar web'
        read(*,*) fr
    sumf=0
c-----------------------------------------------------------------------
c state the fractions for [0] or [theta] or [90] plies in the laminates
c-----------------------------------------------------------------------
    Do while (sumf.NE.1.0)
       write(*,*) 'The sum of the fraction for all plies has to be 1'
       write(*,*) 'Enter the fraction for zero degree plies'
       read(*,*) f0
       write(*,*) 'Enter the fraction for theta plies'
       read(*,*) ftheta
       write(*,*) 'Enter the fraction for 90 degrees plies'
       read(*,*) f90
       sumf=f0+ftheta+f90
    End Do
c---------------------------------------
c determine the reduced stiffnesses at [0]
c---------------------------------------
    v21=v12*E22/E11
    Q11=E11/(1-v12*v21)
    Q12=v12*E22/(1-v12*v21)
    Q22=E22/(1-v12*v21)
    Q66=G12
        Q(1)=Q11
        Q(2)=Q12
        Q(3)=Q22
        Q(4)=Q66
c-----------------------------------------------------
c transform the reduced stiffnesses to different angles
c-----------------------------------------------------
        a=0.0
        call Qmat(a,Q,Qb110,Qb120,Qb220,Qb160,Qb260,Qb660)
        c=90.0
        call Qmat(c,Q,Qb119,Qb129,Qb229,Qb169,Qb269,Qb669)
        d=45.0
        call Qmat(d,Q,Qb115,Qb125,Qb225,Qb165,Qb265,Qb665)
        e=d*pi/180
        Qbar11b=f0*Qb110+ftheta*Qb115+f90*Qb119
        Qbar12b=f0*Qb120+ftheta*Qb125+f90*Qb129
        Qbar22b=f0*Qb220+ftheta*Qb225+f90*Qb229
        Qbar66b=f0*Qb660+ftheta*Qb665+f90*Qb669
```

```
        k11b=Qbar11b-Qbar12b**2/Qbar22b
        k22b=Qbar66b
        a12b=(cos(e))**2-Qbar12b/Qbar22b*(sin(e))**2
        a26b=sin(e)*cos(e)
        hbb=(Nxx/k11b)/eps
        htb=(a12b*Nxx/k11b+a26b*Nxs/k22b)/eps
        if (hbb.LE.htb) then
                thickb=htb
        else
                thickb=hbb
        end if
c-------------------------------------
c determine the properties for the webs
c-------------------------------------
    call Qmat(w,Q,Qb11p,Qb12p,Qb22p,Qb16p,Qb26p,Qb66p)
        call Qmat(-w,Q,Qb11n,Qb12n,Qb22n,Qb16n,Qb26n,Qb66n)
        Qbar11w=(Qb11p+Qb11n)/2
        Qbar12w=(Qb12p+Qb12n)/2
        Qbar16w=(Qb16p+Qb16n)/2
        Qbar22w=(Qb22p+Qb22n)/2
        Qbar26w=(Qb26p+Qb26n)/2
        Qbar66w=(Qb66p+Qb66n)/2
        k11w=Qbar11w-Qbar12w**2/Qbar22w
        k12w=Qbar16w-Qbar12w*Qbar26w/Qbar22w
        k22w=Qbar66w-Qbar26w**2/Qbar22w

        theta=1.0
        betamax=0.0
    Do i=1,90
                theta1=theta*pi/180
        call Qmat(theta,Q,Qb11u,Qb12u,Qb22u,Qb16u,Qb26u,Qb66u)
        call Qmat(-theta,Q,Qb11l,Qb12l,Qb22l,Qb16l,Qb26l,Qb66l)

      Qbar11u=f0*Qb110+ftheta*Qb11u+f90*Qb119
      Qbar12u=f0*Qb120+ftheta*Qb12u+f90*Qb129
      Qbar16u=f0*Qb160+ftheta*Qb16u+f90*Qb169
              Qbar22u=f0*Qb220+ftheta*Qb22u+f90*Qb229
      Qbar26u=f0*Qb260+ftheta*Qb26u+f90*Qb269
      Qbar66u=f0*Qb660+ftheta*Qb66u+f90*Qb669

              Qbar11l=f0*Qb110+ftheta*Qb11l+f90*Qb119
      Qbar12l=f0*Qb120+ftheta*Qb12l+f90*Qb129
      Qbar16l=f0*Qb160+ftheta*Qb16l+f90*Qb169
              Qbar22l=f0*Qb220+ftheta*Qb22l+f90*Qb229
      Qbar26l=f0*Qb260+ftheta*Qb26l+f90*Qb269
      Qbar66l=f0*Qb660+ftheta*Qb66l+f90*Qb669
```

```
      k11u=Qbar11u-Qbar12u**2/Qbar22u
      k12u=Qbar16u-Qbar12u*Qbar26u/Qbar22u
      k22u=Qbar66u-Qbar26u**2/Qbar22u
            k11l=Qbar11l-Qbar12l**2/Qbar22l
      k12l=Qbar16l-Qbar12l*Qbar26l/Qbar22l
      k22l=Qbar66l-Qbar26l**2/Qbar22l
            beta1=k12u**2/(k11u*k22u)
c-------------------------------------------------------
c transform the strains from the xy axis to the angle plies
c-------------------------------------------------------
            a12=(cos(theta1))**2-Qbar12u/Qbar22u*(sin(theta1))**2
            a26=sin(theta1)*cos(theta1)-Qbar26u/Qbar22u*(sin(theta1))**2
c-----------------------
c determine the thickness
c-----------------------
            hb=(Nxx/k11u-Nxs*beta1/k12u)/(eps*(1-beta1))
            ht=((a12/k11u-a26*beta1/k12u)*Nxx+(a26/k22u-a12*beta1/k12u)
     &            *Nxs)/(eps*(1-beta1))
c-------------------------------------------------
c determine the ply that controls the cover thickness
c-------------------------------------------------
            if (hb.GE.ht) then
                  thick=hb
            else
                  thick=ht
            end if
c-------------------------------------
c determine the behavior of the stucture
c-------------------------------------
            Mx=2*Cs*He*Nxs
            My=-Nxx*Cs*He
            c12u=Qbar12u/Qbar22u-(Qbar26u*k12u)/(Qbar22u*k22u)
            c26u=Qbar26u/Qbar22u
            kcu=(2/He)*(c12u*eps+c26u*Nxs/(thick*k22u))
            C44=thick*(((k22u+k22l)*Cs+k22w*(ff+fr)*He)
     &            *(Cs*He/(Cs+He))**2)
            C45=thick*(0.5*(k12u-k12l)*(Cs*He)**2/(Cs+He))
            C55=thick*(0.25*(k11u+k11l)*Cs*He**2)

            betasq=C45**2/(C44*C55)
            if (betamax.LE.betasq) then
                  betamax=betasq
                  thetamax=theta
            end if
            dphi=(C55*Mx-C45*My)/(C44*C55*(1-betasq))
```

```
                Wxx=(C45*Mx-C44*My)/(C44*C55*(1-betasq))
                wgain=(2*thick+(ffw+frw)*thick)/(2*thickb+(ffw+frw)*thick)-1
c-----------------------------------
c write the results to the data files
c-----------------------------------
                write(11,*) theta,betasq,beta1
                write(12,*) thick,hb,ht
                write(13,*) dphi,kcu,Wxx
                write(14,*) theta,hbb,htb
                write(15,*) thickb,wgain
                write(16,*) C44,C45,C55
                theta=theta+1.0
    End Do
        write(*,*) 'Maximum of beta squared at'
        write(*,*) 'theta=',thetamax
        write(*,*) 'max. beta squared=', betamax
    End

c=======================================================
c SUBROUTINE for transfroming reduced stiffness matrix
c=======================================================
    subroutine Qmat(deg,Q,Qb11,Qb12,Qb22,Qb16,Qb26,Qb66)
        implicit none
        real*8 deg,Qb11,Qb12,Qb22,Qb16,Qb26,Qb66,Q(4)
        real*8 Q11,Q12,Q22,Q66,deg1
        intent(in)::deg,Q
        intent(out)::Qb11,Qb12,Qb22,Qb16,Qb26,Qb66
        Q11=Q(1)
        Q12=Q(2)
        Q22=Q(3)
        Q66=Q(4)
        deg1=deg*3.14159/180
        Qb11=Q11*(cos(deg1))**4+2*(Q12+2*Q66)*(sin(deg1))**2
   &    *(cos(deg1))**2+Q22*(sin(deg1))**4
    Qb12=(Q11+Q22-4*Q66)*(sin(deg1))**2*(cos(deg1))**2
   &    +Q12*((sin(deg1))**4+(cos(deg1))**4)
    Qb22=Q11*(sin(deg1))**4+2*(Q12+2*Q66)*(sin(deg1))**2
   &    *(cos(deg1))**2+Q22*(cos(deg1))**4
    Qb16=(Q11-Q12-2*Q66)*sin(deg1)*(cos(deg1))**3+(Q12-Q22+2*Q66)
   &    *(sin(deg1))**3*cos(deg1)
    Qb26=(Q11-Q12-2*Q66)*(sin(deg1))**3*cos(deg1)+(Q12-Q22+2*Q66)
   &    *sin(deg1)*(cos(deg1))**3
    Qb66=(Q11+Q22-2*Q12-2*Q66)*(sin(deg1))**2*(cos(deg1))**2
   &    +Q66*((sin(deg1))**4+(cos(deg1))**4)
        return
        end subroutine Qmat
```

APPENDIX B

PROGRAM FOR LAMINATE ROTATION

Variable and Parameter Definitions

Appendix B is the Fortran 90 program that is used to analyze Laminate Rotation.

The following inputs are required for the program.

Inputs:

Width of the box model, Cs
Height of the box model, H
Elastic properties of the materials used for the box model, E_{11}, E_{22} and G_{12}
Limit strain for the design criterion, ε
Axial loading due to bending, N_{xx}
Load due to torsion, N_{xs}
Configuration of the ply layup – fractions of axial plies, balanced angle plies and transverse plies. Also, the angle for the balanced angle plies, θ.
Orientation for the ply layup of the webs, w
Fraction of the wall thickness for the front spar web, ff
Fraction of the wall thickness for the rear spar web, fr

After inputting the values for the above parameters, the program generates the following outputs.

Outputs:

Bend-twist coupling parameter, β^2
Thickness of the covers, h
Rate of twist, $\phi_{,xx}$
Bending curvature, $W_{,xx}$
Camber curvature, kc
Global stiffnesses, C_{44}, C_{55}, and C_{45}
Relative weight, which is compared to a balanced brenchmark reference of [0] and [45] plies.

Notes: All of the inputs are in degrees and English units.

Program Listing

```
c==============================
c PROGRAM for Laminate Rotation
c==============================
```

```
      Program coupling
      real*8 Cs,He,E11,E22,G12,v12,theta,beta1max
      real*8 sumf,f0,ftheta,f90,v21,Q11,Q12,Q22,Q66,deg1max
      real*8 a,bn,bp,c,e,beta1,C44,C55,C45,k11u,k12u,k22u,Q(4)
      real*8 Qb110,Qb120,Qb220,Qb160,Qb260,Qb660
      real*8 Qb119,Qb129,Qb229,Qb169,Qb269,Qb669
      real*8 Qb11p,Qb12p,Qb22p,Qb16p,Qb26p,Qb66p
      real*8 Qb11n,Qb12n,Qb22n,Qb16n,Qb26n,Qb66n
      real*8 Qb111,Qb121,Qb221,Qb161,Qb261,Qb661
      real*8 Qb112,Qb122,Qb222,Qb162,Qb262,Qb662
      real*8 Qbar11w,Qbar12w,Qbar16w,Qbar22w,Qbar26w,Qbar66w,ffw,frw
      real*8 w,k11w,k12w,k22w,k11l,k12l,k22l,betasq,betasqmax,degsqmax
      real*8 Qfu(3,3),Qfl(3,3),Qbar(3,3),Nxx,Nxs,eps,theta1,thick,h1
      real*8 Mx,My,dphi,c12,c26,cur,kc,N11,N22,N12,thickb,wgain
      real*8 h2,h3,theta2,theta3,s11,s22,s12,s45p,s45n,detA,AI(3,3)
    integer i
c-------------------------------------
c create the data files for the results
c-------------------------------------
      open (unit=11,file='result.dat',status='unknown')
      open (unit=12,file='result1.dat',status='unknown')
      open (unit=13,file='result2.dat',status='unknown')
      open (unit=14,file='result3.dat',status='unknown')
      open (unit=15,file='result4.dat',status='unknown')
    pi=3.14159

    write(*,*) 'Enter the width for the single beam box in inches'
    read(*,*) Cs
    write(*,*) 'Enter its height in inches'
    read(*,*) He
    write(*,*) 'Enter the properties'
    write(*,*) 'E11?'
    read(*,*) E11
    write(*,*) 'E22?'
    read(*,*) E22
    write(*,*) 'G12?'
    read(*,*) G12
    write(*,*) 'v12?'
    read(*,*) v12
      write(*,*) 'strain?'
      read(*,*) eps
      write(*,*) 'Enter the axial load, Nxx'
      read(*,*) Nxx
      write(*,*) 'Enter the shear flow, Nxs'
      read(*,*) Nxs
      sumf=0
```

```
      beta1max=0.0
      betasqmax=0.0
c-----------------------------------------------------------------
c state the fractions for [0] or [theta] or [90] plies in the laminates
c-----------------------------------------------------------------
      Do while (sumf.NE.1.0)
            write(*,*) 'Enter the fraction of zero degree plies'
            read(*,*) f0
            write(*,*) 'Enter the degree for the theta plies'
            read(*,*) theta
            write(*,*) 'Enter the fraction of theta plies'
            read(*,*) ftheta
            write(*,*) 'Enter the fraction of 90 deg plies'
            read(*,*) f90
            write(*,*) 'Enter the angle of the webs'
            read(*,*) w
            write(*,*) 'Enter the fraction for the front spar web'
            read(*,*) ff
            write(*,*) 'Enter the fraction for the rear spar web'
            read(*,*) fr
            sumf=f0+ftheta+f90
      End Do
c---------------------------------------
c determine the reduced stiffnesses at [0]
c---------------------------------------
    v21=v12*E22/E11
    Q11=E11/(1-v12*v21)
    Q12=v12*E22/(1-v12*v21)
    Q22=E22/(1-v12*v21)
    Q66=G12
      Q(1)=Q11
      Q(2)=Q12
      Q(3)=Q22
      Q(4)=Q66
c-----------------------------------------------------
c transform the reduced stiffnesses to different angles
c-----------------------------------------------------
      a=0.0
   call Qmat(a,Q,Qb110,Qb120,Qb220,Qb160,Qb260,Qb660)
      c=90.0
   call Qmat(c,Q,Qb119,Qb129,Qb229,Qb169,Qb269,Qb669)
      bp=theta
   call Qmat(bp,Q,Qb11p,Qb12p,Qb22p,Qb16p,Qb26p,Qb66p)
      bn=-theta
      call Qmat(bn,Q,Qb11n,Qb12n,Qb22n,Qb16n,Qb26n,Qb66n)
      Qbar(1,1)=f0*Qb110+ftheta/2*(Qb11p+Qb11n)+f90*Qb119
```

```
      Qbar(1,2)=f0*Qb120+ftheta/2*(Qb12p+Qb12n)+f90*Qb129
      Qbar(1,3)=f0*Qb160+ftheta/2*(Qb16p+Qb16n)+f90*Qb169
          Qbar(2,1)=Qbar(1,2)
      Qbar(2,2)=f0*Qb220+ftheta/2*(Qb22p+Qb22n)+f90*Qb229
      Qbar(2,3)=f0*Qb260+ftheta/2*(Qb26p+Qb26n)+f90*Qb269
          Qbar(3,1)=Qbar(1,3)
          Qbar(3,2)=Qbar(2,3)
      Qbar(3,3)=f0*Qb660+ftheta/2*(Qb66p+Qb66n)+f90*Qb669
c-----------------------------------
c deterine the properties for the webs
c-----------------------------------
          call Qmat(w,Q,Qb111,Qb121,Qb221,Qb161,Qb261,Qb661)
          call Qmat(-w,Q,Qb112,Qb122,Qb222,Qb162,Qb262,Qb662)
          Qbar11w=(Qb111+Qb112)/2
          Qbar12w=(Qb121+Qb122)/2
          Qbar22w=(Qb221+Qb222)/2
          Qbar16w=(Qb161+Qb162)/2
          Qbar26w=(Qb261+Qb262)/2
          Qbar66w=(Qb661+Qb662)/2
          k11w=Qbar11w-Qbar12w**2/Qbar22w
          k12w=Qbar16w-Qbar12w*Qbar26w/Qbar22w
          k22w=Qbar66w-Qbar26w**2/Qbar22w

          Do i=0,90
                e=i
                theta1=e*3.14159/180
                theta2=theta*3.14159/180
                theta3=-theta*3.14159/180
c-----------------------------------------------------
c transform the stiffnesses into a certain rotation angle
c-----------------------------------------------------
                call Tran(e,Qbar,Qfu)
                call Tran(-e,Qbar,Qfl)
                k11u=Qfu(1,1)-Qfu(1,2)**2/Qfu(2,2)
        k12u=Qfu(1,3)-Qfu(1,2)*Qfu(2,3)/Qfu(2,2)
        k22u=Qfu(3,3)-(Qfu(2,3))**2/Qfu(2,2)
                k11l=Qfl(1,1)-Qfl(1,2)**2/Qfl(2,2)
                k12l=Qfl(1,3)-Qfl(1,2)*Qfl(2,3)/Qfl(2,2)
                k22l=Qfl(3,3)-(Qfl(2,3))**2/Qfl(2,2)
c-------------------------------
c determine the coupling parameter
c-------------------------------
        beta1=k12u**2/(k11u*k22u)
                if (beta1max.LT.beta1) then
                        beta1max=beta1
                        deg1max=e
```

```
                End If
c-------------------------------------------------------------
c transform the fixed stress resultants to the 1-2 coordinate system
c-------------------------------------------------------------
                N11=cos(theta1)**2*Nxx+2*sin(theta1)*cos(theta1)*Nxs
                N22=sin(theta1)**2*Nxx-2*sin(theta1)*cos(theta1)*Nxs
                N12=-sin(theta1)*cos(theta1)*Nxx+(cos(theta1)**2
        &               -sin(theta1)**2)*Nxs

                detA=Qbar(1,1)*Qbar(2,2)*Qbar(3,3)+2*Qbar(1,2)*Qbar(1,3)
        &               *Qbar(2,3)-Qbar(1,3)**2*Qbar(2,2)-Qbar(2,3)**2*Qbar(1,1)
        &               -Qbar(1,2)**2*Qbar(3,3)
                AI(1,1)=(Qbar(2,2)*Qbar(3,3)-Qbar(2,3)**2)/detA
                AI(1,2)=(Qbar(1,3)*Qbar(2,3)-Qbar(1,2)*Qbar(3,3))/detA
                AI(1,3)=(Qbar(1,2)*Qbar(2,3)-Qbar(1,3)*Qbar(2,2))/detA
                AI(2,1)=AI(1,2)
                AI(2,2)=(Qbar(1,1)*Qbar(3,3)-Qbar(1,3)**2)/detA
                AI(2,3)=(Qbar(1,2)*Qbar(1,3)-Qbar(1,1)*Qbar(2,3))/detA
                AI(3,1)=AI(1,3)
                AI(3,2)=AI(2,3)
                AI(3,3)=(Qbar(1,1)*Qbar(2,2)-Qbar(1,2)**2)/detA
c-------------------------------------------------
c compare the strains in different fiber directions
c-------------------------------------------------
                s11=AI(1,1)*N11+AI(1,2)*N22+AI(1,3)*N12
                s22=AI(2,1)*N11+AI(2,2)*N22+AI(2,3)*N12
                s12=AI(3,1)*N11+AI(3,2)*N22+AI(3,3)*N12
                h1=s11/eps
                s45p=cos(theta2)**2*s11+sin(theta2)**2*s22+
        &               sin(theta2)*cos(theta2)*s12
                h2=s45p/eps
                s45n=cos(theta3)**2*s11+sin(theta3)**2*s22+ -
        &               sin(theta3)*cos(theta3)*s12
                h3=s45n/eps
c-------------------------------------------------
c determine the ply that controls the cover thickness
c-------------------------------------------------
                if (h1>=h2 .AND. h1>=h3) then
                        thick=h1
                else if (h2>=h3 .AND. h2>=h1) then
                        thick=h2
                else
                        thick=h3
                end if
                if (e.EQ.0) then
                        thickb=thick
```

```
                end if
c-----------------------------------
c determine the behavior of the structure
c-----------------------------------
                wgain=(2*thick+(ffw+frw)*thick)/(2*thickb+(ffw+frw)*thick)-1
                C44=thick*((Cs*He/(Cs+He))**2)*((k22u+k22l)*Cs
        &               +(ff+fr)*k22w*He)
                C45=0.5*thick*(Cs*He)**2/(Cs+He)*(k12u-k12l)
                C55=0.25*thick*Cs*He**2*(k11u+k11l)
                betasq=C45**2/(C44*C55)
                Mx=2*Cs*He*Nxs
                My=-Nxx*Cs*He
                dphi=(C55*Mx-C45*My)/(C44*C55*(1-betasq))
                cur=(C45*Mx-C44*My)/(C44*C55*(1-betasq))
                c12=Qfu(1,2)/Qfu(2,2)-(Qfu(2,3)*k12u)/(Qfu(2,2)*k22u)
                c26=Qfu(2,3)/Qfu(2,2)
                kc=(2/He)*(c12*eps+c26*Nxs/(thick*k22u))
                if (betasqmax.LT.betasq) then
                        betasqmax=betasq
                        degsqmax=e
                end if
c-----------------------------------
c write the results to the data files
c-----------------------------------
                write(11,*) e,beta1,betasq
                write(12,*) h1,h2,h3
                write(13,*) e,thick,wgain
                write(14,*) dphi,cur,kc
                write(15,*) C44,C45,C55
    End Do
        write(*,*) 'max. beta1'
        write(*,*) deg1max,beta1max
        write(*,*) 'max. betasq'
        write(*,*) degsqmax,betasqmax
    End

c=================================================
c SUBROUTINE for transforming reduced stiffness matrix
c=================================================
    subroutine Qmat(deg,Q,Qb11,Qb12,Qb22,Qb16,Qb26,Qb66)
        implicit none
        real*8 deg,Qb11,Qb12,Qb22,Qb16,Qb26,Qb66,Q(4)
        real*8 Q11,Q12,Q22,Q66,deg1
        intent(in)::deg,Q
        intent(out)::Qb11,Qb12,Qb22,Qb16,Qb26,Qb66
        Q11=Q(1)
```

```
      Q12=Q(2)
      Q22=Q(3)
      Q66=Q(4)
      deg1=deg*3.14159/180
      Qb11=Q11*(cos(deg1))**4+2*(Q12+2*Q66)*(sin(deg1))**2
     &    *(cos(deg1))**2+Q22*(sin(deg1))**4
     Qb12=(Q11+Q22-4*Q66)*(sin(deg1))**2*(cos(deg1))**2
     &    +Q12*((sin(deg1))**4+(cos(deg1))**4)
     Qb22=Q11*(sin(deg1))**4+2*(Q12+2*Q66)*(sin(deg1))**2
     &    *(cos(deg1))**2+Q22*(cos(deg1))**4
     Qb16=(Q11-Q12-2*Q66)*sin(deg1)*(cos(deg1))**3+(Q12-Q22+2*Q66)
     &    *(sin(deg1))**3*cos(deg1)
     Qb26=(Q11-Q12-2*Q66)*(sin(deg1))**3*cos(deg1)+(Q12-Q22+2*Q66)
     &    *sin(deg1)*(cos(deg1))**3
     Qb66=(Q11+Q22-2*Q12-2*Q66)*(sin(deg1))**2*(cos(deg1))**2
     &    +Q66*((sin(deg1))**4+(cos(deg1))**4)
      return
      end subroutine Qmat
c=============================================================
c SUBROUTINE for tranforming laminate into rotation angle
c=============================================================
      subroutine Tran(d1,Qbar,TR2)
      implicit none
      real*8 d1,d,Qbar(3,3),TR1(3,3),TR2(3,3)
      intent(in)::d1,Qbar
      intent(out)::TR2
      d=d1*3.14159/180
      TR1(1,1)=Qbar(1,1)*(cos(d))**2+Qbar(1,2)*(sin(d))**2
      &            -Qbar(1,3)*2*sin(d)*cos(d)
      TR1(1,2)=Qbar(1,1)*(sin(d))**2+Qbar(1,2)*(cos(d))**2
      &            +Qbar(1,3)*2*sin(d)*cos(d)
      TR1(1,3)=Qbar(1,1)*sin(d)*cos(d)-Qbar(1,2)*sin(d)*cos(d)
      &            +Qbar(1,3)*((cos(d))**2-(sin(d))**2)
      TR1(2,1)=Qbar(2,1)*(cos(d))**2+Qbar(2,2)*(sin(d))**2
      &            -Qbar(2,3)*2*sin(d)*cos(d)
      TR1(2,2)=Qbar(2,1)*(sin(d))**2+Qbar(2,2)*(cos(d))**2
      &            +Qbar(2,3)*2*sin(d)*cos(d)
      TR1(2,3)=Qbar(2,1)*sin(d)*cos(d)-Qbar(2,2)*sin(d)*cos(d)
      &            +Qbar(2,3)*((cos(d))**2-(sin(d))**2)
      TR1(3,1)=Qbar(3,1)*(cos(d))**2+Qbar(3,2)*(sin(d))**2
      &            -Qbar(3,3)*2*sin(d)*cos(d)
      TR1(3,2)=Qbar(3,1)*(sin(d))**2+Qbar(3,2)*(cos(d))**2
      &            +Qbar(3,3)*2*sin(d)*cos(d)
      TR1(3,3)=Qbar(3,1)*sin(d)*cos(d)-Qbar(3,2)*sin(d)*cos(d)
      &            +Qbar(3,3)*((cos(d))**2-(sin(d))**2)
```

```
TR2(1,1)=TR1(1,1)*(cos(d))**2+TR1(2,1)*(sin(d))**2
&               -TR1(3,1)*2*sin(d)*cos(d)
TR2(1,2)=TR1(1,2)*(cos(d))**2+TR1(2,2)*(sin(d))**2
&               -TR1(3,2)*2*sin(d)*cos(d)
TR2(1,3)=TR1(1,3)*(cos(d))**2+TR1(2,3)*(sin(d))**2
&               -TR1(3,3)*2*sin(d)*cos(d)
TR2(2,1)=TR1(1,1)*(sin(d))**2+TR1(2,1)*(cos(d))**2
&               +TR1(3,1)*2*sin(d)*cos(d)
TR2(2,2)=TR1(1,2)*(sin(d))**2+TR1(2,2)*(cos(d))**2
&               +TR1(3,2)*2*sin(d)*cos(d)
TR2(2,3)=TR1(1,3)*(sin(d))**2+TR1(2,3)*(cos(d))**2
&               +TR1(3,3)*2*sin(d)*cos(d)
TR2(3,1)=TR1(1,1)*sin(d)*cos(d)-TR1(2,1)*sin(d)*cos(d)
&               +TR1(3,1)*((cos(d))**2-(sin(d))**2)
TR2(3,2)=TR1(1,2)*sin(d)*cos(d)-TR1(2,2)*sin(d)*cos(d)
&               +TR1(3,2)*((cos(d))**2-(sin(d))**2)
TR2(3,3)=TR1(1,3)*sin(d)*cos(d)-TR1(2,3)*sin(d)*cos(d)
&               +TR1(3,3)*((cos(d))**2-(sin(d))**2)
return
end subroutine Tran
```

Appendix II

Brett Sikola's
MS Project

2004

Linear Modeling of Aeroelastic Twist of a High Aspect Ratio Wing with Significant Taper

Brett Sikola, Lawrence W. Rehfield

Abstract

The most significant aeroelastic deformation that occurs in optimized cruise flight is the elastic twist that occurs about the spanwise direction of the wing. By shifting the distribution of the spanwise aerodynamic loads, this aeroelastic twist can have a negative impact on induced drag and structural loading. Hence preliminary design tools that can characterize this twist, particularly in cases of significant spanwise taper such as presented in this paper, are important for beginning the design of efficient aircraft with such wings.

The preliminary design tool presented here makes several simplifying assumptions. Airfoil sections are assumed to behave linearly in both an elastic sense and a sectional aerodynamic sense. As this is primarily a structural tool, aerodynamic behavior is further simplified to assume that individual airfoil sections are assumed to not affect each other in the spanwise direction (Trefftz plane). This is classical "strip theory aerodynamics" that has been used for high aspect ratio lifting surfaces for generations. Furthermore, with composite construction that is balanced with respect to a spanwise axis, the axis serves as an elastic axis (EA) which permits bending and torsion to be elastically uncoupled. Emphasis is placed here, therefore, on elastic twist. Simple, but rational and familiar, design criteria are utilized to size the wing.

Nomenclature

EA = Elastic Axis

$c_a(r)$ =Root Aerodynamic Chord

λ =Taper Ratio

q =Dynamic Pressure

y_{ac} =Chordwise Separation Distance of the Center of Pressure and EA

c_l =2-D Coefficient of Lift

a_0 =2-D Lift Slope of Airfoil

c_m =Constant Coefficient of Moment

c_{lturn} =2-D Coeffecient of Lift Under Turning Conditions

f_s =Factor of Safety

k11 =Axial Reduced Stiffness per Unit Thickness

k22 =Torsional Reduced Stiffness per Unit Thickness

Introduction

Aeroelastic response is difficult to assess in preliminary design. Many of the tools used to predict aeroelastic response are difficult to use or require large run times (such as ANSYS multi-physics engine runs or a NASTRAN run) and hence are limited mostly to final analysis rather than true parametric optimization of an aeronautical structure.

It is the intent of this work to present an alternative means of simultaneous aerodynamic/structural analysis of high aspect ratio tapered aerodynamic structures loaded normal to their spanwise structural axis that can not only give a realistic first

scaling of the necessary thicknesses of structural box skinning material, but also of its subsequent deformation. This formulation is also applicable to swept wings, as only the component of the airflow normal to the wing need be considered as causing aerodynamic loading, as is commonly done in preliminary swept wing analysis. Further, and most importantly, the taper of the wings need not be constant or continuous in any sense, so long as a leading edge normal chord can be specified at any point along the span.

Methodology

The geometric parameters of the wing (or other lifting surface), and its structural composition, must first be described. Secondly, appropriate candidate structural concepts and material systems must be identified.

The material system later illustrated makes use of composite materials, but isotropic materials may easily be used. In the case of anisotropic materials, such as carbon-composite, reduced stiffnesses must be calculated for laid up plies in a manner consistent with sectional analysis[1]. Also the design strain limit must be specified, a common design limit[2]. Finally, the minimum manufacturable wall thickness of the material must be established based upon experience.

The subsequent example and discussion only describes the method for a linear taper, but as long as all the parameters can be given as either explicit functions or points that may be interpolated, the methodology can be applied. Currently, many wing dimensions are reduced dimensions or ratios taken from other dimensions. For the current example, the root chord, $c_a(r)$, the taper ratio of tip chord divided by root aerodynamic

chord, λ, and the wing half-span. It is assumed that the internal structure scales equivalently with the external aerodynamic structure. Consequently, the dimensions of the wing structure box must be given at the root, including the thickness of the vertical webs. The webs are often sized as a fraction of the thickness of the upper and lower covers based upon experience and transverse shear flow. It is assumed that the wing structure box is more or less rectangular and a closed section. While the global structure is a tapered prism, the individual finite element sections are modeled as untapered. As the bending and twisting deformations are elastically uncoupled, aeroelastic twist can be estimated independently[3].

The structural material is a 50/50 mix of [0] degree spanwise plies and [±45] torsionally stiff plies, i.e. $[0_2, \pm 45]$, composed of AS4/3501-6 composite material. This laminate mimics the F/A-18 and AV-8B without chordwise plies and gives a fairly good compromise between bending and twisting stiffness[1].

The dynamic pressure is the only dimensional aerodynamic loading parameter, q. The dimensionless aerodynamic loading parameters are the sectional aerodynamic parameters: the coefficient of lift at cruise (1-g) loads, c_l, the lift slope of the section, a_0, the perceived maximum multiple of 1g that will be experienced in turns, and the angle-of-attack independent coefficient of moment, c_m. The inclusion of the c_m is a departure from the earlier work of Reference 4., in addition to several other extensions made here of that work.

The separation of the quarter chord from the elastic center of the structural box is given as y_{ac}. Finally the factor of safety, f_s, is used to multiply the maximum g-loading to provide for reasonable design margin.

As one last convergence parameter, the number of elements used in the analysis must be specified. A consideration of the convergence of the solution is given subsequently.

The analysis of the aerodynamic structure makes use of a series of aerodynamic independent sections that interact elastically along the EA. There is one degree of elastic freedom per element, twisting about the spanwise axis. Each element experiences a load at its outboard tip (node) and twists elastically according to this load. The outboard load and the applied aerodynamic load, based on both the initial c_l the induced angle of attack times a_0, are applied at the inboard station (node). The amount of elastic twist experienced by each element under the load applied to it is based on its sectional torsional stiffness, itself dictated by the structural box and the stiffnesses of the material system. In order to remain consistent with this model, the torsional displacement of the inboard node (wing root) of the innermost element is fixed at zero (c_l stays at its original value), while the load applied to the outboard node of the most outboard element is set to zero; hence this element sees no relative elastic displacement. The loadings just described can also be seen below in Fig.1.

A system of linear equations results from the equilibrium of the global structure. Note that only the twisting moment about the spanwise axis is considered in the displacement of the system; while the system does displace in bending parallel with the c_l loading, the impact on the aerodynamic load distribution is minor, and, hence, it is only considered in the context of the bending design strain limit. Once the nodal displacements have been found, all of the resultant loadings can be found.

In the entire system implemented in the coming example, the loadings are actually found three times. In the first run, no displacements are allowed and the bending loads are found for the worst case scenario of the maximum g-loading multiplied times the factor of safety. These are then used in conjunction with the calculated bending stiffness to find the skin thickness necessary to reach the bending strain limit at the root[1]; the minimum thickness is also enforced at this step in order to ensure manufacturability.

In the second run, the loads are calculated in a manner similar to the thickness determination loads, only now the c_l is reflective of cruise conditions. These loads are used as a baseline for comparison with the loads that are found in the elastically displaced case. The final case, of course, finds the loads produced in the wing that has elastically deformed to its loads.

One final interesting calculation that is carried out is the divergence speed estimation. By holding constant the dynamic pressure used to calculate the skin thickness but varying the dynamic pressure used to calculate the elastic twist of the wing, the displacement of the outer tip of the wing can be found as a function of dynamic pressure and speed. Thus, the divergence speed can be found graphically by finding where the transverse displacement asymptotically approaches infinity. In the following example, the result of this calculation is compared to the typical 70-75% chord calculation[5].

Example Structure

The example considered in this paper is the wing of a Reno Unlimited Class Air Racer outlined in a preliminary design study and illustrated in Fig. 2. The Reno airport at the time of the Reno air races is generally at about nine thousand feet real altitude, and

competitive racers in the unlimited class generally race at about 644 to 724 km/h (400 to 450 M.P.H.), which sets the dynamic pressure. The rest of the pertinent data for the racer are listed Table 1. Note that the sign convention for the twist is positive nose up. Although the taper of this wing is constant, the methodology is still general enough to analyze a wing of arbitrary taper, as mentioned earlier.

Results and Discussion: Reno Air Racer

1. As is visible in Fig.3, the combination of the separation of the coefficient of lift from the aerodynamic and the negative coefficient moment results in the negative coefficient of moment ultimately pushes the induced angles of attack negative. Due to aeroelastic effects, the section lift coefficient has decreased by about 0.018, a decrease of about 15%. This seems unlikely to cause radical problems, but there is certainly a perturbation from any initially "rigid" optimized wing configuration. Further notice the two inflection points of the twist distribution of the wing. The inboard inflection point is mostly the result of the non-constant thickness of the section; otherwise the loading tends to scale proportionally to the stiffness with the current scaling. The second inflection point is a result of the requirement that the rate of change of the twist will reach zero at the outboard section, as this section is free of twisting loads.
2. The twisting load certainly seems affected by the aeroelastic deformation, reducing it by about twelve percent, visible in Fig.4. While the twist does not

directly affect performance, it is interesting to note its decrease and resulting impact on the balance of the aircraft.

3. The bending moment is less affected by the change in sectional angle of attack, with a reduction in overall lift in the wing less than 10%, as seen in Fig.5. The qualitative curve exhibits no dramatic shift from its original shape. This same trend is seen in a relatively minor 1.6" shift in the spanwise center of pressure.
4. The minimum manufacturability criterion was triggered slightly before the half-span mark, visible in Fig. 6. From the sole perspective of rigid bending loads it would seem that very small thicknesses would be all that would be required to avoid the strain limit in the outboard sections of the wing; however, not including the manufacturability requirement produced unrealistic and undesirable outboard displacements. It is seen, therefore, that reducing the minimum manafacturable thickness would not necessarily save any appreciable weight.
5. As expected, the torsional and bending stiffness scale with both the span and the stiffness, as is evident from the kink at about half-span in Fig. 7. Notice that both never reach zero, as this would produce infinite tipwise displacements and loads, neither of which is realistic.
6. As the loading is initially only $2/15^{th}$'s that of the turn conditions that set the thickness, it is not surprising that the strain remains far below the 4500 microstrain limit set for the material, visible in Fig. 8. Had the wing been held rigid, the strain would have been constant for the initial inboard section. Clearly the strains have been lessened due to the induced angles of attack of the sections.

Note that once the strain was no longer held constant it drops off rapidly; hence the strain limit is not reach in the outboard sections.

7. In a comparison of the current models estimate of the divergence speed with that of the 70-75% section model, both predict divergence at flight speeds over 100 M.P.H. (160 km/h) faster than that of the anticipated flight envelope, as seen in fig. 9. By both estimates then it would seem that the current structural configuration is a good initial estimate for preventing divergence.

Convergence Study

As is common with lower order elements, such as those with only two nodes, a large number of nodes are required to achieve satisfactory convergence; in this case of the order of 100. Additionally the outermost element is a fairly gross estimation when the elements are fairly large, and in fact one can almost draw a line connecting the kinks in the station twists that are created by the final rigid element. It would seem logical to conclude that holding the last element to a certain much smaller fraction the size of the other elements would increase accuracy for the same computational cost.

Conclusions

The preliminary design tool presented in this paper can clearly provide useful feedback in the preliminary design of elastic high aspect ratio wings of arbitrary taper. By this code alone it can be reasonably construed that many higher order models of the aerodynamic performance on "rigid" airframes, such as CFD and wind tunnel analysis,

might fail to fully predict the behavior of the structure, and may be unwarranted without including aeroelastic coupled effects.

From the specific case in question, several other conclusions may be drawn. Depending on the magnitude of the coefficient of moment and the coefficient of lift, the elastic response of the wing may induce positive or negative changes in the angle of attack. The traditional 70-75% span model for divergence prediction is more conservative for this illustration. Structural rigidity towards the wingtips is generally not as important at preventing failure of the material as keeping deformations and changes in load under control. It may also be noted here that by setting the sectional aerodynamic coefficients of the outer part of the wing corresponding to control surfaces and to values consistent with a control input, control reversal may also be modeled.

It is the intention of this preliminary design methodology to allow for analysis of more diverse planforms than that analyzed here, and, as designed it can be easily applied to a host of other lifting surfaces uncoupled elastic bend-twist response. Finally it runs in only a few seconds on almost any desktop computer running Matlab.

Final Remarks

What is new?

1. Analysis efficiency – suitable for preliminary design or conceptual structural design on desktop computers
2. Simple, but rational, established, and validated modeling approach.

3. Illustration – extreme taper of wing, realistic parameter values for aircraft type, minimum gauge drives design of outboard wing sections (helps reduce tip twist and outboard elastic twist effects)
4. Valid only for wing covers with balanced ply layups.

References

1. Cheung, R. H., "Some Strategies for Creating Bend-Twist Coupling in Box Beams," MS Thesis, University of California, Davis, 2002.
2. Rehfield, L.W., EAE-135, Aerospace Structures (Class Notes), University of California Davis, 2002
3. Megson, T.H.G., Aircraft Structures for Engineering Students, Edward Arnold (Publishers) Ltd., London, 1980
4. Chang, Y.S., Analysis and Design Methodology for Chordwise Deformable Wings, PhD Dissertation, University of California Davis, 1993
5. Bisplinghoff, R.L. and Ashley, H., Priniciples of Aeroelasticity, Dover Publications, Inc., New York, 1962.

Appendix: Matlab Code

Source Matlab code for design methodology

Tables

Quantity	Value	Units
q	$19.6*10^3(2.848)$	(Pa)lb/in^2
$c_{a(r)}$	1.122(44.19)	m(inches)
Wing box width at root	$0.4* c_a(r)$	m(inches)
Wing box height at root	$0.1* c_a(r)$	m(inches)
y_{ac} at the root	$0.2* c_a(r)$	m(inches)
Wing half span	2.925(115.6)	m(inches)
c_l	0.12	-
a_0	5.7	-
c_m	$-3.22*10^{-2}$	-
c_{lturn}	$5* c_l$	-
f_s	1.5	-
λ	0.39	-
k11	$81.5*10^9(11.*10^6)$	Pa(lbf/in^2)
k22 box covers	$21.34*10^6(3.095*10^6)$	Pa(lbf/in^2)
k22 vertical box members	$35.58*10^6(5.16*10^6)$	Pa(lbf/in^2)
vertical box members fraction	0.4	-
microstrain criteria	0.0045	m/m(in/in)
minimum thickness	$1.27*10^{-3}(0.05)$	m(inches)

Table 1, Design Data for Example Reno Air Racer

Figures

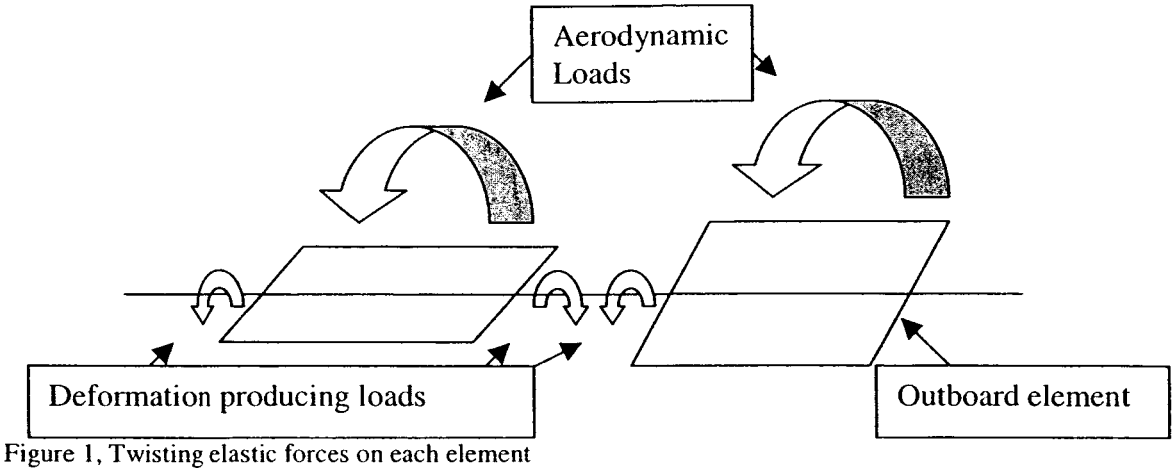

Figure 1, Twisting elastic forces on each element

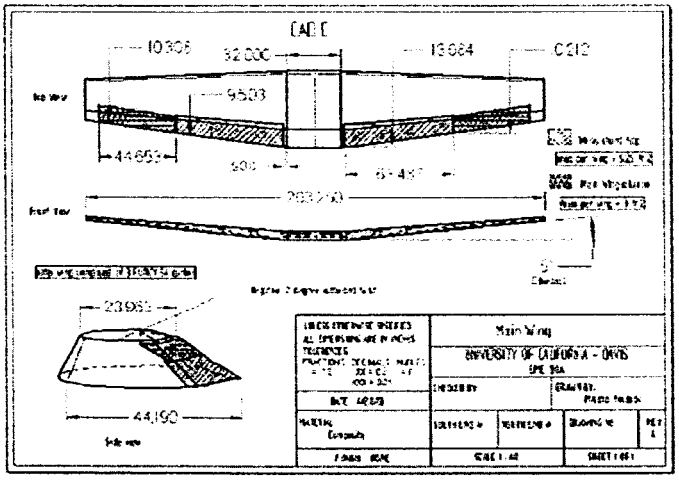

Figure 2, Example Reno Air Racer Wing Planform

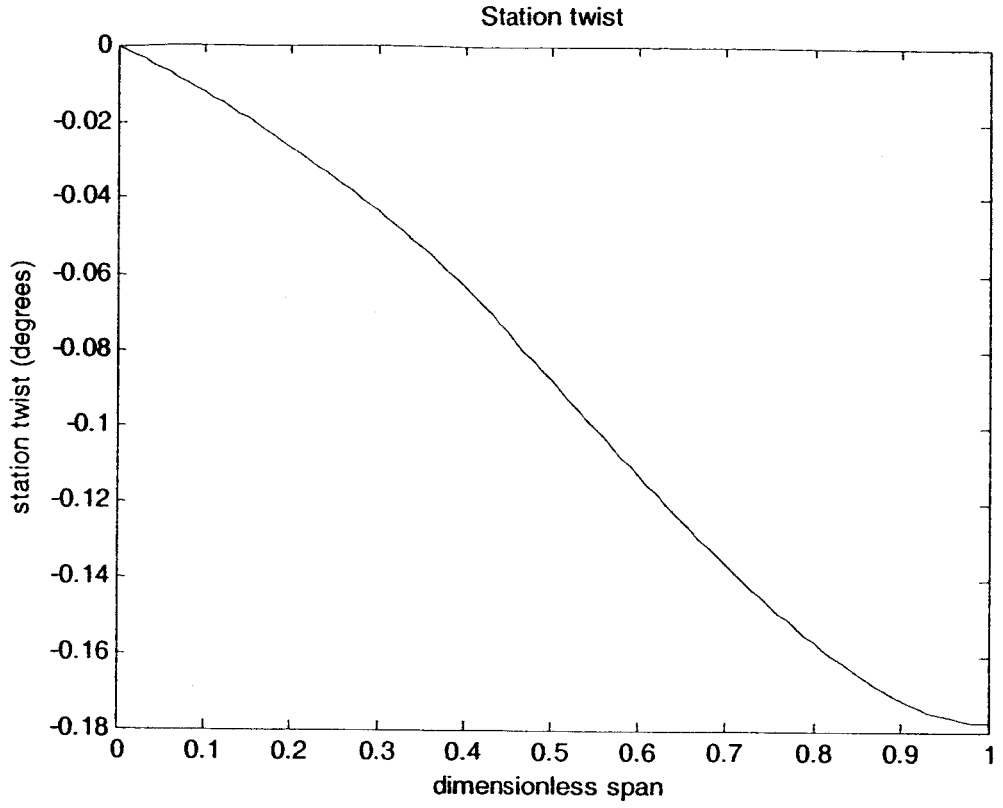

Figure 3, Station Twist

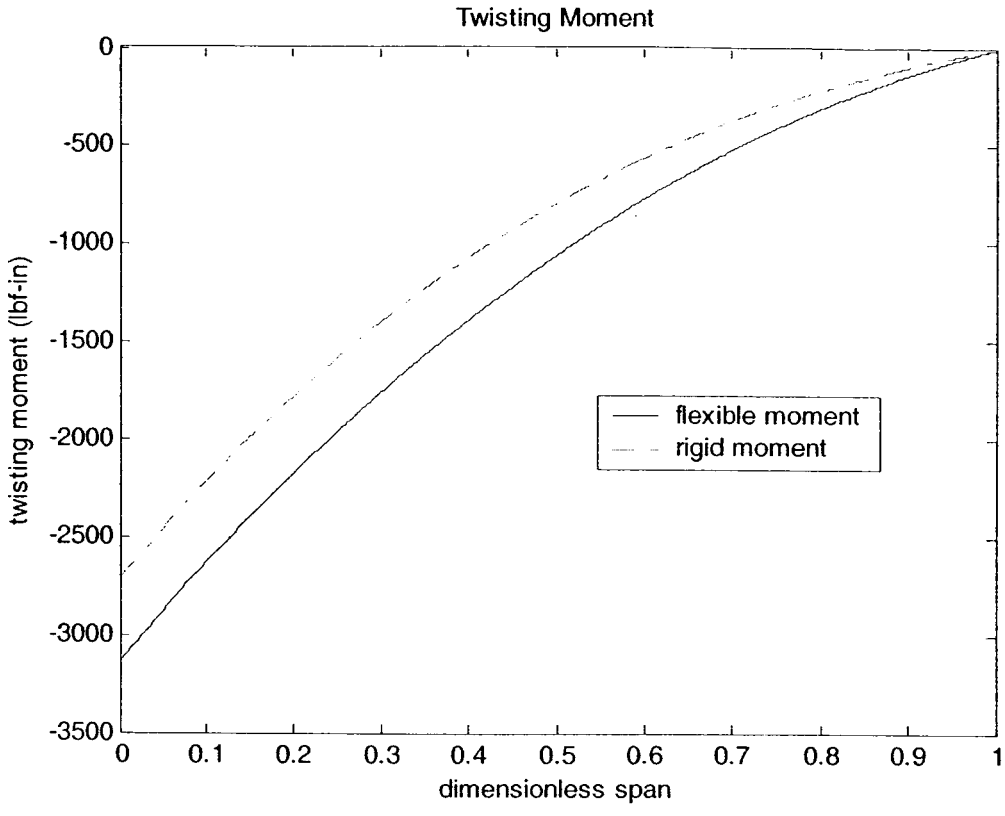

Figure 4, Twisting Moment

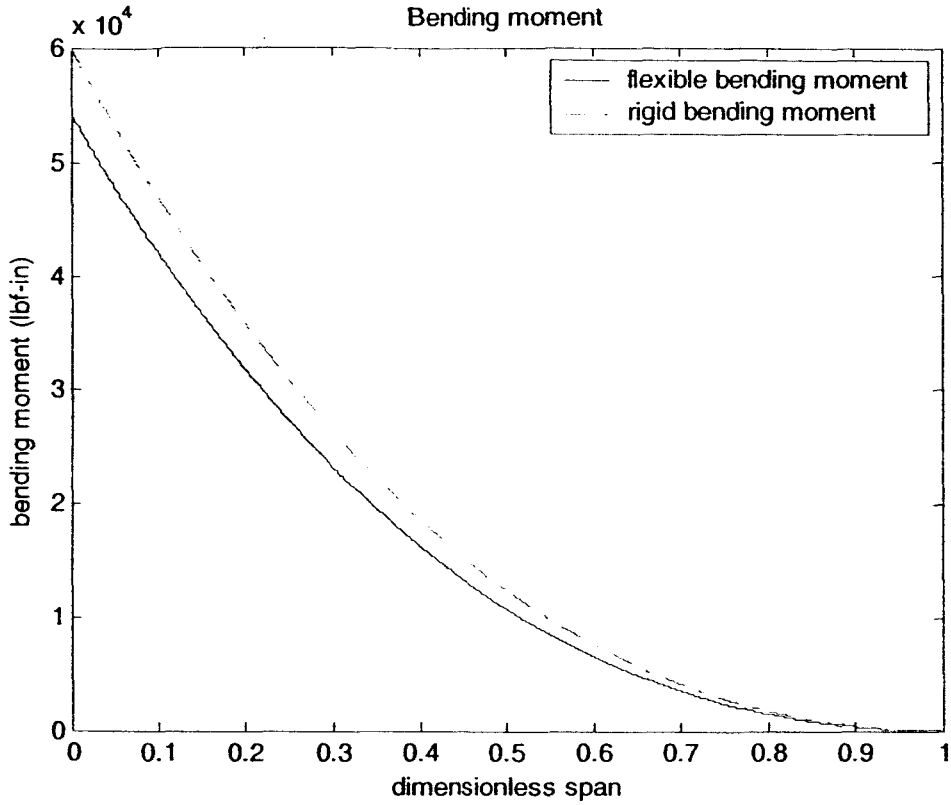

Figure 5, Bending Moment

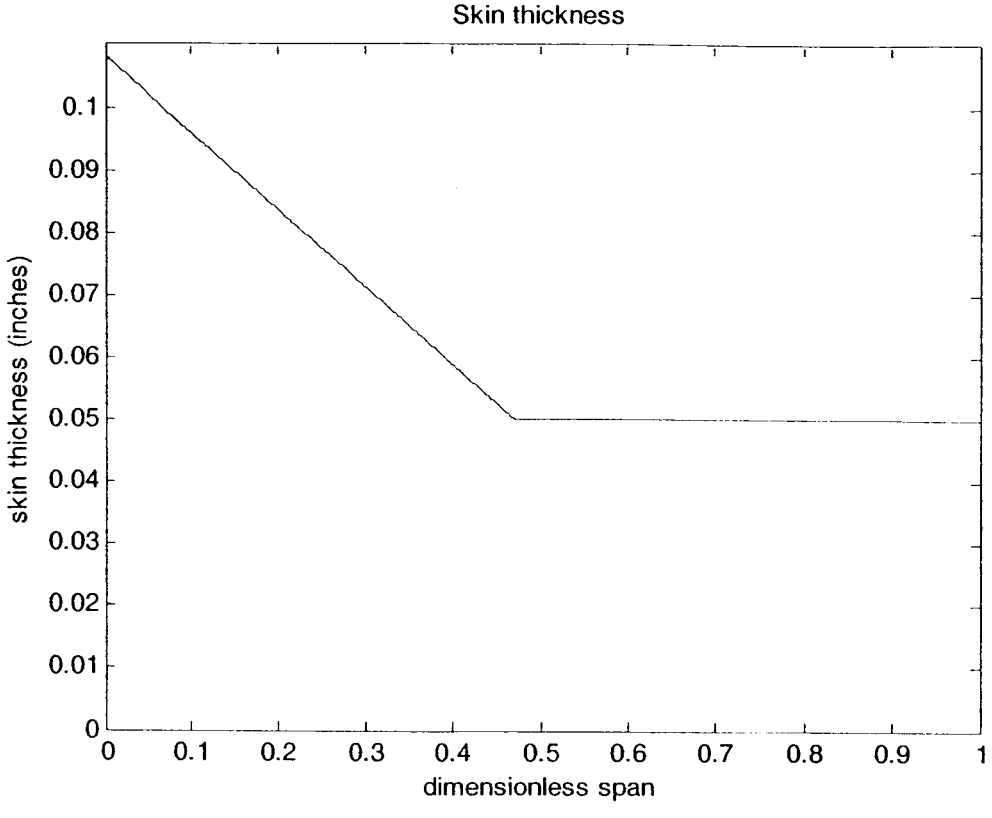

Figure 6, Skin (Cover) Thickness

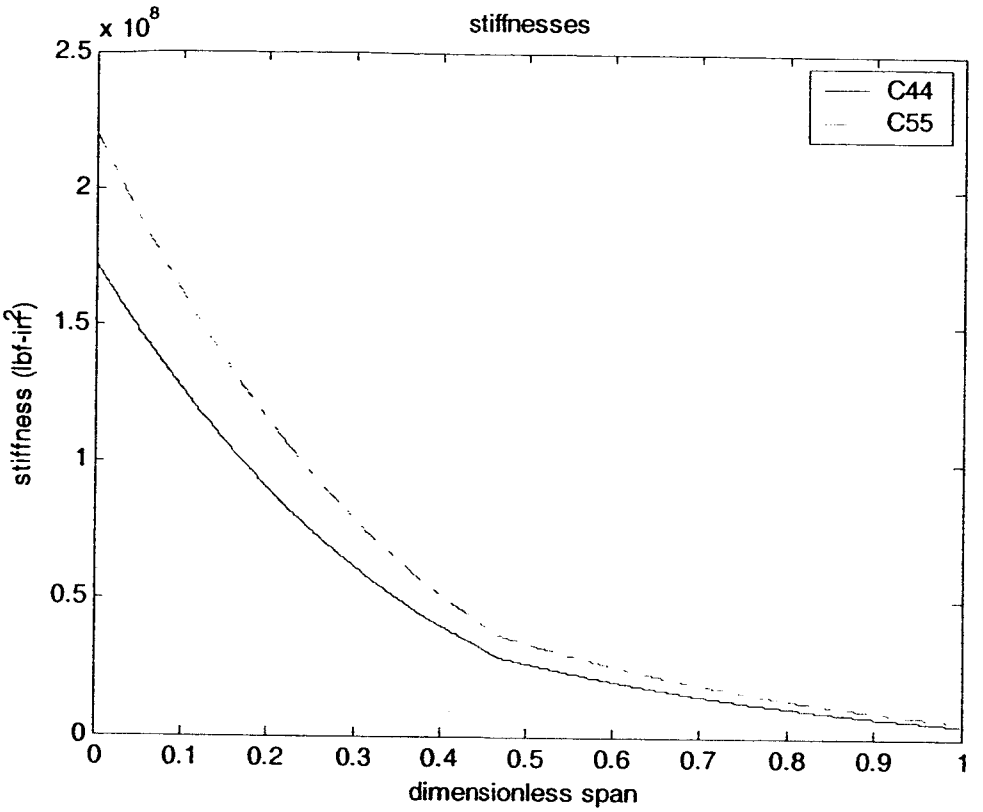

Figure 7, Stiffnesses

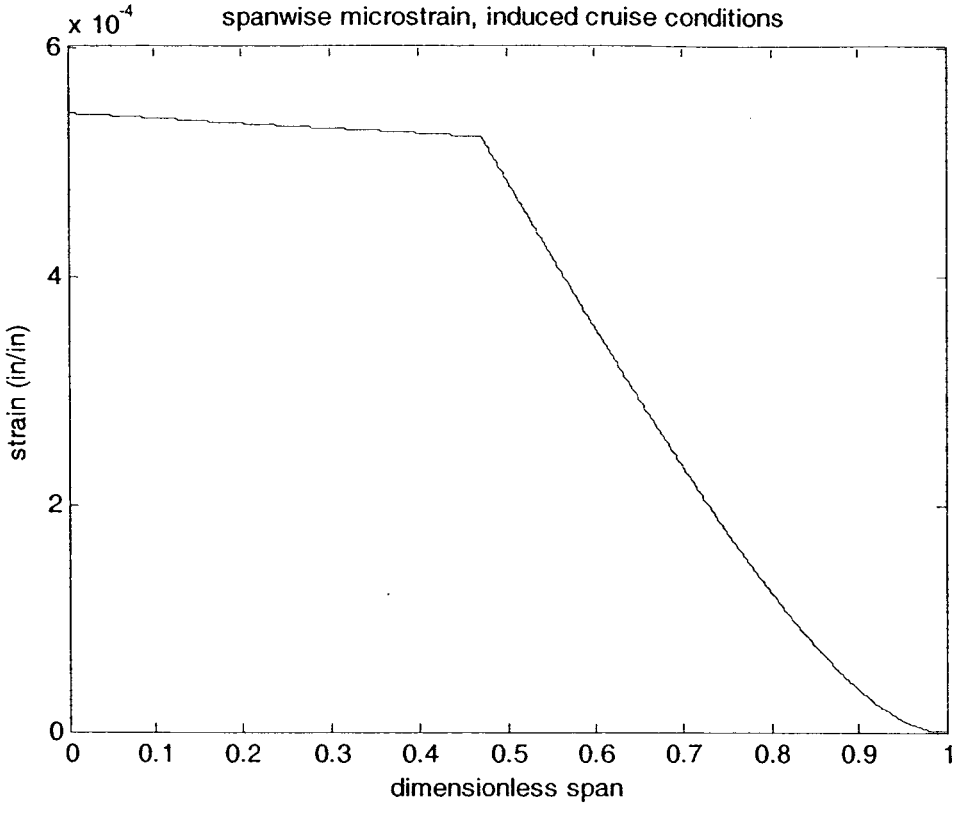

Figure 8, Spanwise Microstrain under Cruise Conditions

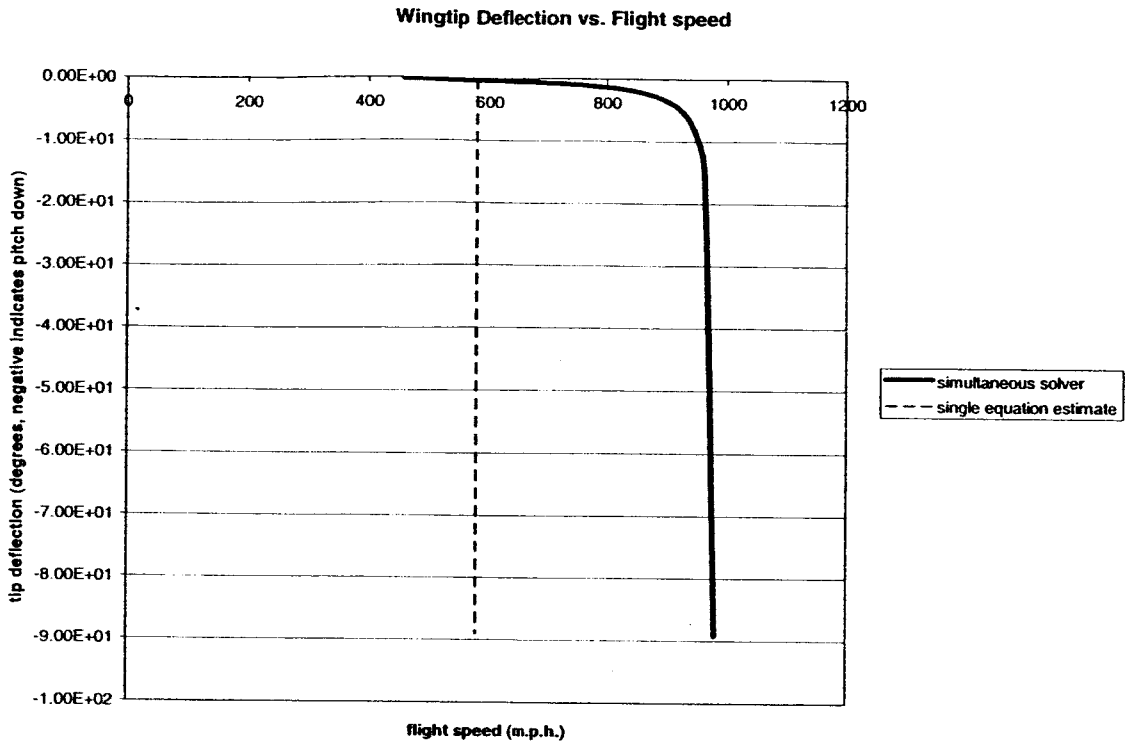

Figure 9, Torsional Divergence Prediction

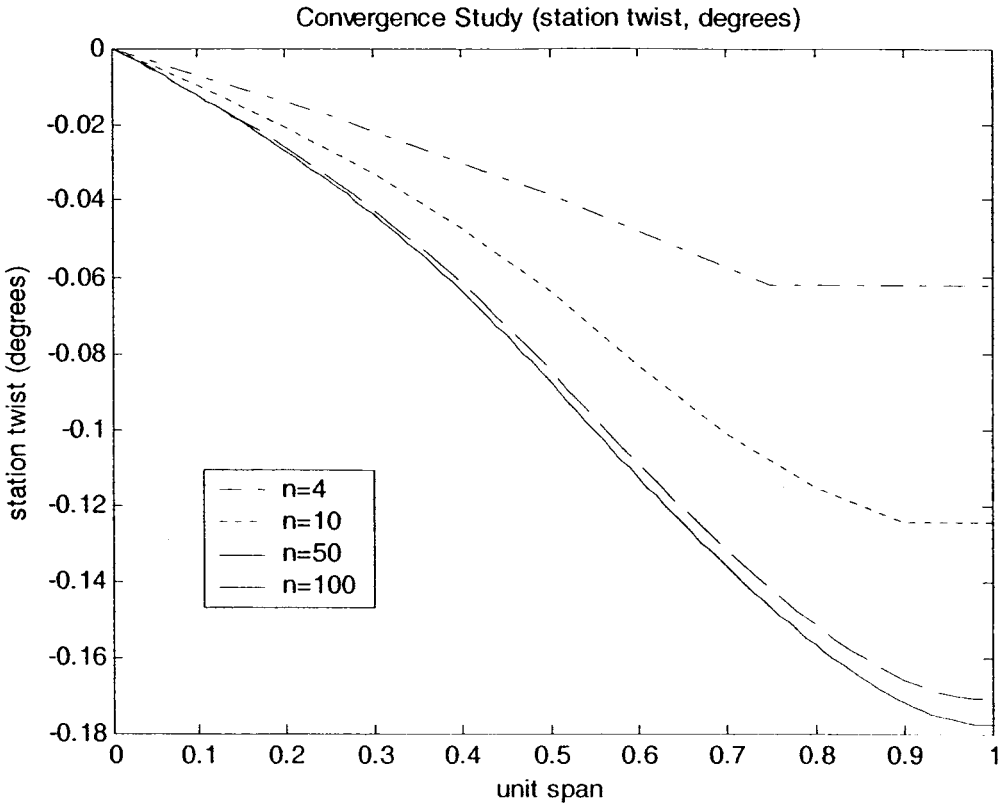

Figure 10, Convergence Study

```
%Brett Sikola
%NASA funded wing twist approximation
%initial debug matlab convergence study
clear all
%close all
format short e
clc


%first the geometry and the loading must be defined
%a linear taper will be assumed; dimensions in inches and lbs

taper_ratio=.39  ;               %dimensionless, between 1 and 0
root_aero_chord=44.190  ;              %inches
root_cover_height=.1*root_aero_chord ;             %inches
root_cover_length=.4*root_aero_chord   ;           %inches
root_y_ac=.2*root_aero_chord   ;                         %inches
wing_half_span=115.6250  ;              %inches
S=wing_half_span*(root_aero_chord+root_aero_chord*taper_ratio)/2 ; %in^2

q=2.848 ;                              %lb/in^2
ao=5.7 ;                               %dimensionless (lift slope)

cm=-3.22e-2;                           %dimensionless (cm, assumed span-wise constant)
cl=.12;                               %dimensionless (assumed to be constant, may curve fit ↙
 later)

cl_turn= 5*.12 ;                          %dimensionless, commonly reached value (not ideal ↙
 coordinated)
fs = 1.5       ;                    %dimensionless, factor of safety (1.5 for manned vehicl ↙
es)

k11=11.82e6   ;              %lbf/in^2 (axial stiffness)
k22=3.095e6   ;                      %lbf/in^2  (shear stiffness)
k22web=5.16e6  ;                     %lbf/in^2  (shear stiffness of the webs alone)
webf=0.4       ;                     %dimensionless (web thickness as fraction of cover th ↙
ickness)
microstrain=4500 / 1e6   ;            %allowable microstrain (note pure strain conversion)
h_min=.05          ;                    %inches, dictated by manafacturability of uncoup ↙
led plies


n=100  ; %input('enter the number of elements, 2 or greater');
l=wing_half_span/n ;                %individual segment length, constant

a=zeros(n,1);                  %create empty matrices that the do loop
b=a;, c=a;, d=a;               %and end conditions fill
y_ac=a;, ca=a;, cs=a;, H=a;, C44=a;, scale=a;,mom=a;

%begin specifying the three diagonals of the matrix
%the b vector is the diagonal entries,
%while the a and c vetors are the diagonals to the left and right, respectively
%the d matrix is the remainder matrix

%coeffecient scaling loop; these will later be used to fill the a,b,c,d vectors
for i=1:n
    scale(i)= 1-(1-taper_ratio)*((i-1)/n + 1/2/n) ;  %as all linear dimensions scale prop ↙
```

```
ortionally
    y_ac(i)=scale(i)*root_y_ac;                    %they will be scaled using a value
    ca(i)  =scale(i)*root_aero_chord;               %calculated at each segment
    cs(i)  =scale(i)*root_cover_length;
    H(i)   =scale(i)*root_cover_height    ;
 end

%%%%%%%%%%%%%%%%%%%%%%%%%%%%%%%%%%%%%%%%%%%%%%%%%%%%%%%%%%%%%%%%%%%%%%%%%%%%%%%
%%%%%%%%%find h using minimum manafacturability and turn bending (rigid)%%%%%%%%
%%%%%%%%%%%%%%%%%%%%%%%%%%%%%%%%%%%%%%%%%%%%%%%%%%%%%%%%%%%%%%%%%%%%%%%%%%%%%%%

lift_turn(1)=q*ca(1)*l*( cl_turn*fs ) ;
for i=2:n
    lift_turn(i)=q*ca(i)*l*( cl_turn*fs );                          %rigid segmentary l ↙
ifting
end

shear_turn(n)=lift_turn(n);
for i=(n-1):-1:1
    shear_turn(i)=lift_turn(i)+shear_turn(i+1);    %rigid segment rootside shearing moment
end

bend_turn(n)=1/2*l*lift_turn(n);
for i=(n-1):-1:1
    bend_turn(i)=bend_turn(i+1)+1/2*l*lift_turn(i)+l*shear_turn(i+1) ; %rigid bending mom ↙
ent
end

for i=1:n
   h(i)=bend_turn(i)/(k11*H(i)*cs(i)*microstrain);   %needed bending stiffness calculation
   if h(i) < h_min
       h(i)=h_min ; %enforce minimum thickness
   end
end

%%%%%%%%%%%%%%%%%%%%%%%%%%%%%%%
%vector of thicknesses complete%
%%%%%%%%%%%%%%%%%%%%%%%%%%%%%%%

%fill out 'd' matrix, torque forces that are constant regardless of aoa
for i=1:n
    d(i)=(cl*y_ac(i)+cm*ca(i))*ca(i)*q*l;
end

%%%%%%%%%%%%%%%%%%%%%%%%%%%%%%%
%%%%%%%% rigid cruise case %%%%%
%%%%%%%%%%%%%%%%%%%%%%%%%%%%%%%

mom_rigid(n)=d(i) ;
for i=(n-1):-1:2
    mom_rigid(i)=d(i) + mom_rigid(i+1);                  % rigid twisting moment
end
mom_rigid(1)=d(1)+mom_rigid(2) ;

lift_rigid(1)=q*ca(1)*l*cl ;
for i=2:n
    lift_rigid(i)=q*ca(i)*l*cl;                        %rigid segmentary lifting
```

```
end
total_lift_rigid=sum(lift_rigid);

shear_rigid(n)=lift_rigid(n);
for i=(n-1):-1:1
    shear_rigid(i)=lift_rigid(i)+shear_rigid(i+1);    %rigid segment rootside shearing mo ↙
ment
end

bend_rigid(n)=1/2*l*lift_rigid(n);
for i=(n-1):-1:1
    bend_rigid(i)=bend_rigid(i+1)+1/2*l*lift_rigid(i)+l*shear_rigid(i+1) ; %rigid bending ↙
 moment
end

cp_rigid=bend_rigid(1)/shear_rigid(1);                %center of pressure, rigid

%%%%%%%%%%%%%%%%%%%%%%%%%%%
%% end rigid cruise case %%
%%%%%%%%%%%%%%%%%%%%%%%%%%%

% find sectional stiffnesses %

for i=1:n
   C44(i)=cs(i)^2*H(i)^2/(cs(i)+H(i))^2*(2*h(i)*k22*cs(i) + 2*h(i)*webf*k22web*H(i)) ;
   C55(i)=2*h(i)*k11*cs(i)*H(i)^2/4 ;
end


% fill out a,b,c vectors %

for i=3:n
    a(i)=-C44(i-1)/l;          %a(1) and a(2) are zero
end

b(1)=1;
for i=2:(n-1)
    b(i)=( C44(i-1)+C44(i) )/l - ao*ca(i)*q*y_ac(i)*l;   %note special end conditions
end
b(n)=C44(n-1)/l - ao*ca(n)*q*y_ac(n)*l;

for i=1:(n-1)
    c(i)=-C44(i)/l;    %c(n)=0 as its original value was retained
end

%solve a,b,c,d tri-diagonal matrix (i.e. strictly 3 banded sparse matrix)%
torque_alphas=tridiag(a,b,c,d) ;

%% Reduce data from the elastic simultaneous case %%

mom(n)=d(n) + ao*ca(n)*q*y_ac(n)*l*torque_alphas(n) ;
for i=(n-1):-1:2
    mom(i)=d(i) + ao*ca(i)*q*y_ac(i)*l*torque_alphas(i) + mom(i+1);  % induced twisting m ↙
oment
end
mom(1)=d(1)+mom(2) ;
```

```
lift(1)=cl*q*l*ca(1)  ;
for i=2:n
    lift(i)=q*ca(i)*l*(cl+ao*torque_alphas(i))   ;          % induced segmentary lifting
end
total_lift=sum(lift);

shear(n)=lift(n);
for i=(n-1):-1:1
    shear(i)=lift(i)+shear(i+1);                % induced segment rootside shearing moment
end

bend(n)=1/2*l*lift(n);
for i=(n-1):-1:1
    bend(i)=bend(i+1)+1/2*l*lift(i)+l*shear(i+1) ;  % induced bending moment
end

cp=bend(1)/shear(1);                                    % induced center of pressure

%%%%% failure criteria, microstrain and divergence %%%%
for i=1:n
    strain(i)=bend(i)/(k11*H(i)*cs(i)*h(i));   %needed bending stiffness calculation
end



x_alphas=[0 1/n:1/n:(1-1/n) 1];
x=1/2/n : 1/n : (1-1/2/n) ;

q_td=qtd(x,n,C44,y_ac,l,S,ao)

%%%%%%%%%%%%
%PLOT OUTPUT%
%%%%%%%%%%%%


figure(1) %alphas
torque_degrees=torque_alphas*180/pi ;
torque_degrees(n)
y=[0 ;torque_degrees(2:n); torque_degrees(n)];
plot(x_alphas,y);
xlabel('dimensionless span');, ylabel('station twist (degrees)');, title('Station twist');

figure(2)%twisting moment
plot(x,mom,x,mom_rigid,'-.') ;
legend('flexible moment','rigid moment') ;
title('Twisting Moment')
xlabel('dimensionless span');
ylabel('twisting moment (lbf-in)');

figure(3) %shear
plot(x,shear,x,shear_rigid,'-.') ;
legend('flexible shear','rigid shear') ;
title('Shear')
xlabel('dimensionless span');
ylabel('shear (lbf)');

figure(4)  %bending moment
```

```
plot(x,bend,x,bend_rigid,'-.') ;
legend('flexible bending moment','rigid bending moment') ;
title('Bending moment')
xlabel('dimensionless span');
ylabel('bending moment (lbf-in)');

figure(5)  %h, thickness
plot(x,h) ;
title('Skin thickness')
xlabel('dimensionless span');
ylabel('skin thickness (inches)');

figure(6)  %C44, C55
plot(x,C44,x,C55,'-.') ;
legend('C44','C55') ;
title('stiffnesses')
xlabel('dimensionless span');
ylabel('stiffness (lbf-in^2)');

figure(7)  %microstrain
plot(x,strain)
title('spanwise microstrain, flexible case')
xlabel('dimensionless span')
ylabel('strain (in/in)')

%%%%%%%%%
%- end -%
%%%%%%%%%
```

```
function [result]=tridiag(a,b,c,d)

%gauss-jordan tri-diag solver

%declare an intermediate matrix to which solutions will begin
%being written.  Declare size of matrix to speed execution
m=length(d);
bb=zeros(m,1);
cc=bb;
dd=bb;
result=bb;
%the first row is unaffected by the row ops that eliminate the
%front row in the first loop, so write it in
bb(1)=b(1);
cc(1)=c(1);
dd(1)=d(1);

%the first loop eliminates the front row by taking the row above it
%and multiplying it by a value that would make it the same as the leading
%entry in the next row, and then subtracting with this modified row
for j=2:m
    bb(j)=b(j)-(a(j)/bb(j-1))*cc(j-1);
    cc(j)=c(j)                        ;
    dd(j)=d(j)-(a(j)/bb(j-1))*dd(j-1);
end

%this leaves one equation in one unknown in the last row, which is solved
%explicitly
result(m)=dd(m)/bb(m);
%the row above it then becomes defined, and this is carried through the
%remainder of the equations, solving the tri-diagonal system
for j=m-1:-1:1
    result(j)=(dd(j)-cc(j)*result(j+1))/bb(j);
end
```

```
function [result]=qtd(x,n,C44,y_ac,l,S,ao)

%find station at closest to  .75 dimensionless span

found=0;

for i=1:n
    test=x(i);
    if test > 0.70
        if found == 0
            answeri=i ;
            found = 1 ;
        end
    end
end

Kinverse=1/C44(1) ;
for i=2:answeri
    Kinverse=1/C44(i)+Kinverse ;
end
K=1/Kinverse ;

result=K/S/y_ac(answeri)/ao ;
```